Doctoral Dissertation

# Fabrication of Monolithic Materials Based on Poly(vinyl alcohol) and Their Applications

ポリビニルアルコールを基盤とするモノリスの
合成と応用

Xiaoxia Sun

January 2014

Department of Applied Chemistry
Graduate School of Engineering,
Osaka University

# Contents

## General Introduction

The last two decades have witnessed an emerging and rapidly increasing interest in the development of monolithic material. The monolith is considered as an outstanding functional material in both academic and industrial applications, and has been utilized widely in various fields, due to its unique open-cellular three-dimensional (3D) interconnected porous structure in a single piece, precise control size of flow-through channels and depth of pores as well as high mechanical property derived from continuous phase.

There has been a very long developmental process of monolithic materials taking place since the early 1960s, with theoretical discussions on the benefits of such porous gel structure for chromatographic application recorded in the early 1950s [1]. Kubín et al. were the first to fabricate a 2-hydroxyethyl methacrylate hydrogel material with low crosslinking degree in order to replace beaded polymers or inorganic oxides. Nevertheless, this kind of material did not have high permeability and allowed only relatively low flow rate [2]. In the early 1970s polyurethane foam fabricated by in situ polymerization was the first monolithic material used as columns for liquid and gas chromatography [3-5]. However, it did not find any resonance within the chromatographic community. Afterwards, a compressed continuous bed with good permeability at a high flow rate was prepared consisting of acrylic acid and N,N-methylene bis(acrylamide) in the presence of a salt in an aqueous medium. This material did not appear to be a real monolith, because it had a particulate character and only the compression afforded the desired monolith-like structure [6, 7]. Thus, the legitimate “monolithic age” starts at the verge of the 1990s. In 1992, the term of

“monolith” was firstly introduced in the literature by Svec and Frèchet. Monolithic blocks of porous highly crosslinked polymers were obtained by copolymerizing glycidyl methacrylate and ethylene dimethacrylate mixed with porogenic solvent in a mold. After modification, the material was highly permeable and allowed the very fast separations of proteins [8-10]. Later, in the middle of 1990s, Tanaka et al. studied the silica-based monolith as separation media for reversed-phase liquid chromatography with controlled porous properties [11-13]. Afterwards, monoliths have been studied and applied in numerous areas.

Compared to other porous media like porous membranes and porous particles which are also commonly investigated, monoliths possess unique characteristics such as fast mass transfer based on low pressure loss, high resolution because of uniform structure without void, high capacity derived from large surface area, various matrix polymers, easy chemical modification to graft functional groups, suppression of nonspecific adsorption due to neutral polymer structure, and low shear forces by monolith structure (Figure 1) [14-17].

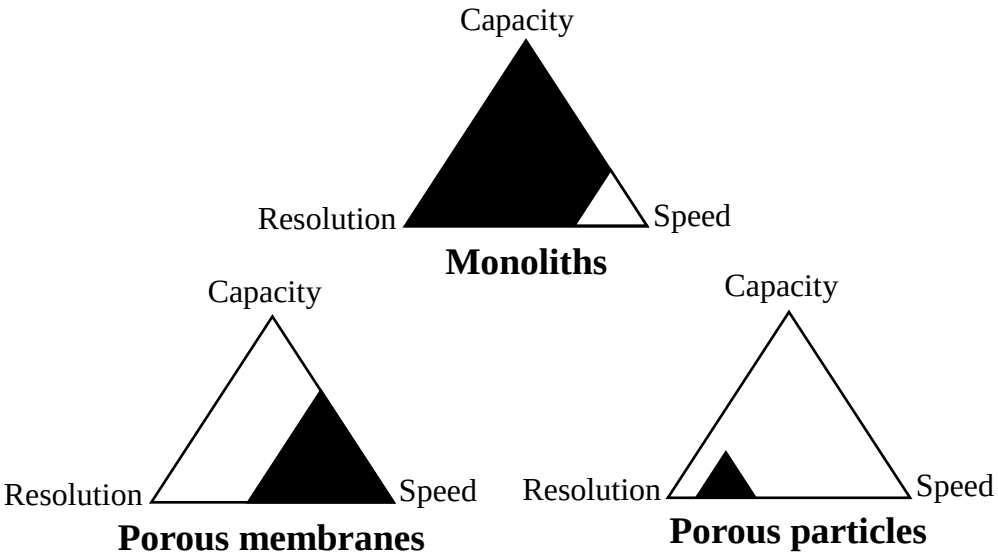


**Figure 1.** Advantages of monoliths for application of stationary phases in separation field

Separation matrix in separation and filtration techniques is one of the most common applications for monolith. As far as we know, particle packed columns have been used as stationary phases for a long time. However, the advent of small particles and small dimension columns result in an increase in hydraulic resistance of the column, thereby increasing the analysis time and necessitating the use of high pressure pumps. Besides, the low mass transfer and poor permeability are also the defects for the particle packed columns [18, 19]. Monoliths with the large through-pore structure in a whole piece afford good bed permeability and mass transfer, providing high flow rate at moderate backpressure. Therefore, it is regard as an ideal candidate to separate large and small molecules such as pretein [20, 21], double stranded DNA [22], peptides [23], cells, polymer-supported reagent and scavengers [24]. Up to present, monolithic supports have been widely used in capillary HPLC [25-27], GC [28], capillary electrochromatogrphy [29], thin layer chromatography [30], and solid phase extraction SPE [31].

Since the first monolithic structures were used in chromatography, monoliths are for many people synonymous with columns. However, less is known about a wide variety of other applications which are also fit for monoliths, such as carriers for immobilization of enzymes [32-34], tissue engineering [35], static mixers [36], as well as thermally responsive gates and valves [37-39]. Use of monolithic supports for enzyme immobilization has rapidly expanded recently. Immobilized enzymes are now finding applications in a wide variety of areas, such as biotechnology, chemical synthesis, and so on [40-42]. In the past, particles were predominantly used as supports for immobilization of enzymes [43, 44]. However, monoliths have recently become an attractive alternative due to their unique properties, including better accessibility of the

active site for substrates, very low back pressure, stability in most solvents, and versatility of functional group available on the pore surface of the monoliths. Besides, ease of preparation in any size and shape is another significant advantage of them.

In general, monoliths can be categorized into two types: polymer-based monolith and silica-based monolith. Figure 2 shows example scanning electron micrographs of silica-based and organic polymer-based porous monoliths [45, 46]. Silica monolith possesses a well defined network of both macro- and meso-pores, while polymer monolith generally only has macroporous structure.

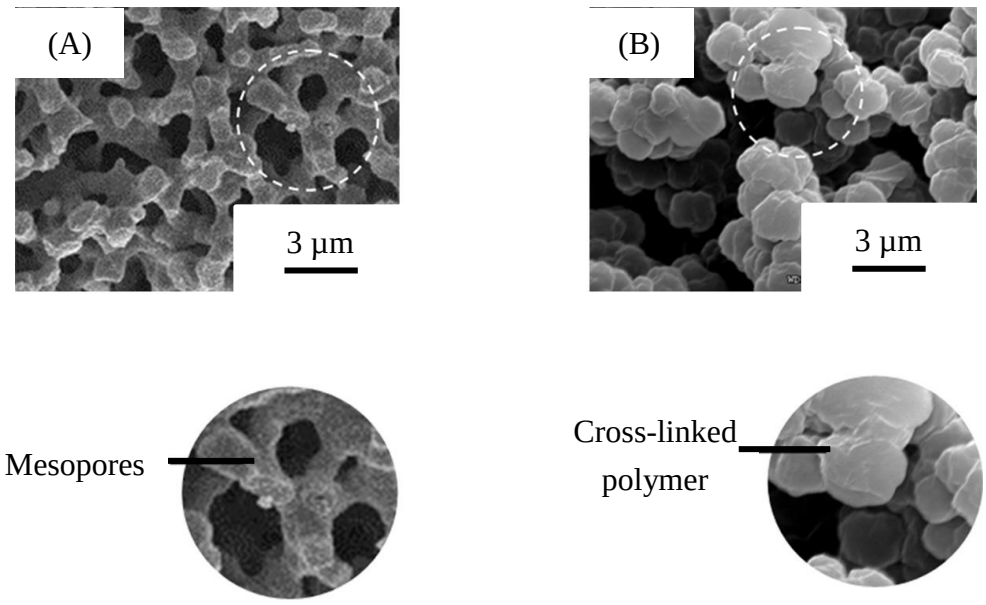


**Figure 2.** SEM images of (A) silica-based monolith and (B) polymer-based monolith

The preparation of silica monolith is often a multi-step procedure [47-49]. A sol-gel step is involved to determine the feature and domain size of a macroporous flow-through-pore structure. Followed by a solvent exchange step, an intra-skeleton

mesopore space is created [50, 51]. Tetramethoxysilane and tetraethoxysilane are the most commonly used as starting materials for the fabrication of silica-based monoliths (Figure 3) [52, 53]. Silica-based monoliths have good solvent resistance, high mechanical stability, high surface area and column efficiency. However, they can be only operated in the range of pH 2-8 for any substantial period of time and can be degraded rapidly in certain mobile phases, which limit their further applications [54].

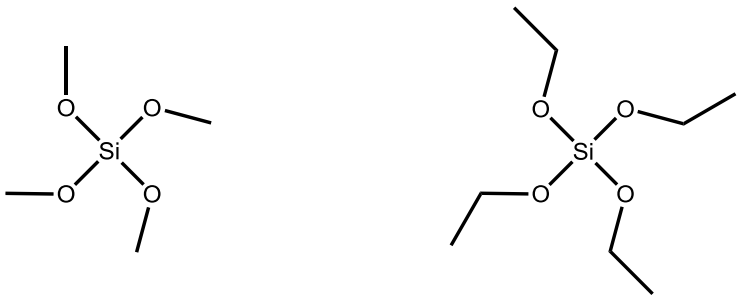


**Figure 3.** Representative starting materials for silica-based monoliths

In contrast, polymer-based monoliths have gradually occupied an impressively strong position because of their good biocompatibility and high chemical stability over a wide pH range. Additionally, the surface property and functionality of polymer-based monoliths can be easily controlled by proper selection of various polymers and their modifications. Figure 4 shows some regular monomers with different functional groups used for polymer-based monolith [55].

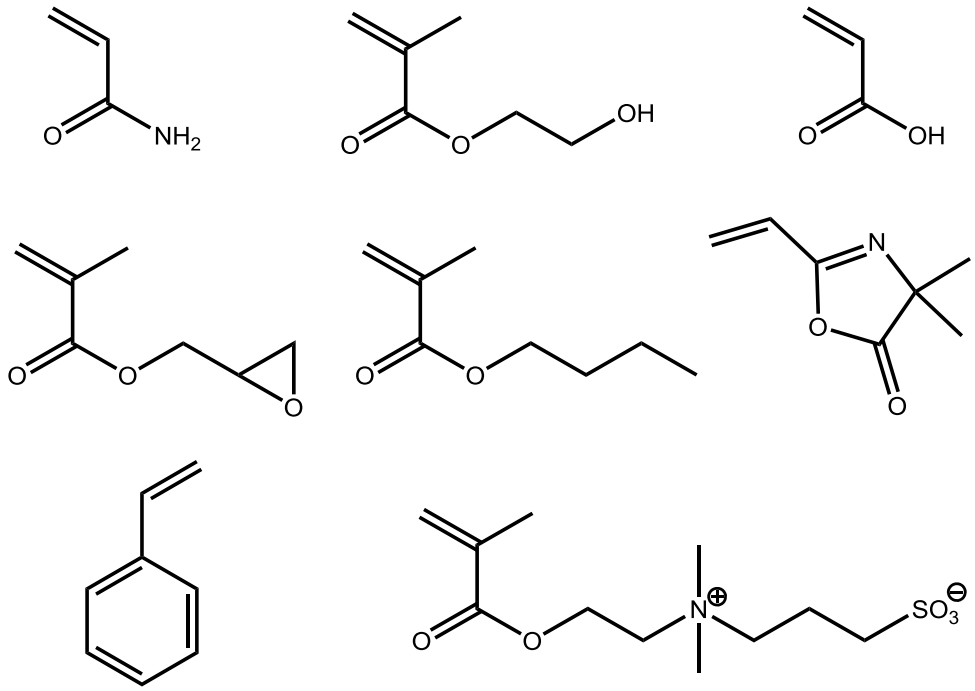


**Figure 4.** Examples of monomers used for the preparation of porous polymer-based monoliths

To date, significant progress has been made to the preparation of polymer-based monolith. There has been a variety of methods reported to produce polymer-based monoliths from corresponding monomers by classical free-radial polymerization processes with thermal or UV initiation, polymerizations using high energy radiations (γ-rays and electron beam irradiation), controlled/living polymerizations, high internal phase emulsion method and polycondensation reaction [56].

Thermally initiated free radical polymerization is the first approach to fabricate rigid polymer-based monolith. This method is simple and developed from suspenstion polymerization which is typically applied in the preparation of porous beads. Compared

to the suspension polymerization used for the preparation of beads, the polymerization for the preparation of monolith in an unstirred mold is different because of the lack of interfacial tension between the aqueous and organic phases, and the absence of hynamic forces which are typical of stirred dispersions. The porous properties are controlled by the polymerization temperature, selection of porogens, crosslinking monomers and polymerization time [57-59].

Photoinitiation is developed in the arena of monoliths in 1997. A mixture similar to that of thermally initiated method is introduced in the mold and irradiate with UV light to initiate the polymerization. Compared to thermally initiate polymerization, this method is significantly faster even at room temperature and can be finished in minutes. Besides, the porogens with low boiling temperature can also be used such as methanol, ethanol, ethy acetate, and hexane. However, the photoinitiated monoliths showed twice as high back pressure thus revealing a difference in the porous structure [60-63].

The polymerization method using high energy radiation such as γ-rays and electron beam irradiation do not need an initiator and can be carried out at any temperature and in almost any container including stainless steel tubes. The ionizing radiation creates ions and a large amount of free radicals to initiate the polymerization reactions. The reaction mechanism is free radical polymerization. For this method, the dose rate plays an important role in the control of final porous structure of monolith. The higher dose rate can create more free-radicals to accelerate the polymerization and crosslinking, resulting in larger pore structure [64]. A certain drawback of this method is that the use of γ-rays is dangerous to the scientists, and electron beam is applied as a high energy alternative to it.

To obtain better control of porous properties of polymer monolith, living

polymerization is developed. In this process, the chain termination and chain transfer reaction are absent and the rate of chain initiating is much larger than that of chain propagation. And a fast and quantitative reaction of an initiator or catalyst with monomers can create all potentially growing polymer chains at the same time. Therefore the polymer chains can grow at a constant rate to form the very similar length, which would result in a better homogenous structure control of the monoliths. The most typical control/living polymerizations include nitroxide-mediated polymerization, organotellurium-mediated living radical polymerization, atom transfer radical polymerization and ring-opening metathesis polymerization [65, 66].

Polymerized high internal phase emulsion (polyHIPE) which is firstly reported by Unilever Research [67] and the more detailed report is published by Small et al [68, 69], is another new method to fabricate polymer monolith. HIPE is a kind of emulsion system with extremely high volume ratio of internal phase or dispersed phase (above 74%). During the fabrication process, monomers in the organic phase are polymerized surrounding the droplets created by internal aqueous phase, forming holes that connect the discrete droplets and creating a continuous aqueous phase. After removing the internal aqueous phase, the monoliths are obtained with open-cellular interconnected pore structure. Moreover, in the polyHIPE, the monomer concentration is very low which make the polymerization heat can be dissipated easily, leading to the formation of large pores.

Polycondensation which is also called step-growth polymerization is another contribution to the family of methods enabling the preparation of monoliths. In this process, the chain end is repeated activated and allows for growth of all polymer chains in the system no matter how long they are. In comparison to free-radical polymerization,

this method is not sensitive to oxygen and the procedure of de-aeration is not needed [70, 71].

Recently, the author's laboratory has developed a new technique to fabricate polymer-based monoliths by phase separation method. This method consists of thermally induced phase separation method (TIPS) and non-solvent induced phase separation method (NIPS), both of which just use polymer itself as the precursor instead of monomers. Very recently, another new method called thermally impacted non-solvent induced phase separation (TINIPS) is developed on the basis of NIPS method. This process of this method is similar to that of NIPS method, but moreover introduces a thermal factor. In the previous work, through the TIPS method, polymethylmethacrylate (PMMA) and polyacrylonitrile (PAN) monoliths have been farbricated successfully [72, 73]. The fabrication process for PMMA monolith is shown as Figure 5. PMMA resin is dissolved in a mixture of solvent (ethanol) and non-solvent (water) by heating at 60 °C, followed by cooling to 20 °C, leading to the formation of the macroporous polymer monolith. During the cooling step, the phase separation of the polymer solution takes place to form the PMMA monolith with high surface area and uniform porosity without using any template.

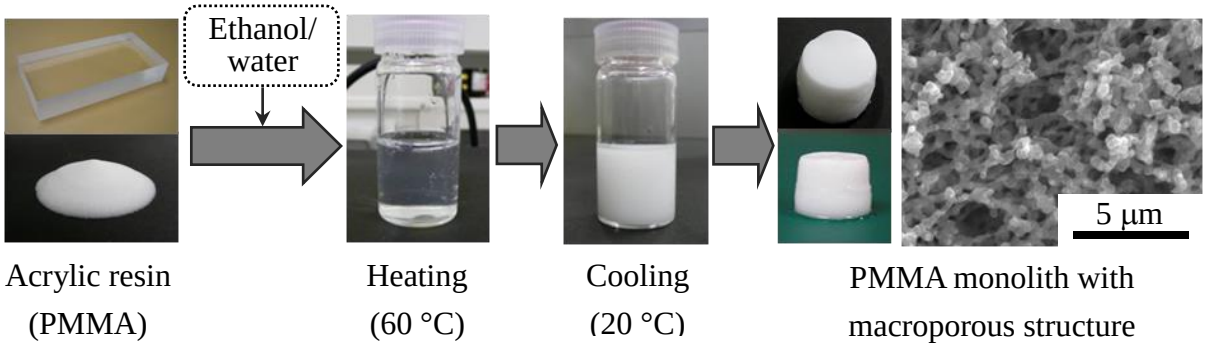


**Figure 5.** Fabrication process of PMMA monolith through TIPS method

By the NIPS method, polycarbonate (PC) monolith is fabricated successfully [74]. Figure 6 shows the synthesis procedure of PC monolith. PC powder is dissolved completely in $CHCl_3$ (solvent) at 60 °C for 30 min. After cooling to room temperature, cyclohexane (non-solvent) is added in 5 min. Afterwards, the solution is kept at 20 °C and the phase separation takes place after a few minutes to form the monolith. The solvent in the monolith is then replaced with ethanol for 3 times. Finally the obtained monolith is dried in vacuum.

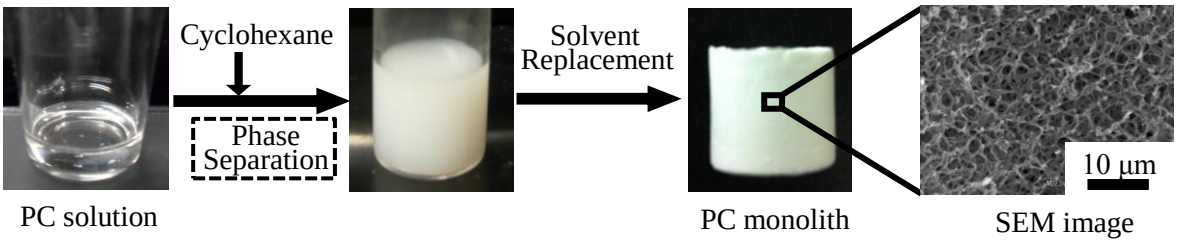


**Figure 6.** Fabrication process of PC monolith through NIPS method

Compared to conventional polymerization methods, both of TIPS and NIPS are simple, fast and energy-saving fabrication methods with high level of control over the pore size and its distribution. Moreover, this kind of methods is template-free, which means the shape of the monoliths can be modified by altering the shape of the vessel. Up to now, there are many kinds of polymer-based monoliths already fabricated through phase separation method in the author's laboratory. Their properties and possible applications are listed in Table 1.

**Table 1.** Properties and possible applications of polymer-based monoliths fabricated through phase separation method

| Polymers | Properties | Possible Applications |
|---|---|---|
| Acrylic Resin | Chemical modification<br>Solvent resistance | Separation matrix<br>Catalyst matrix |
| Poly(acrylonitrile) | Heat resistance<br>Solvent resistance | Precursor for battery material<br>Separation matrix |
| Polyolefin | Heat resistance<br>Solvent resistance | Battery separator<br>Matrix for fuel gas |
| Polycarbonate | Hydrophobic<br>Solvent resistance | Ion remavol<br>Separation matrix |
| Poly(lactic acid) | Biodegradability<br>Biocompatibility | Agriculture material<br>Biomaterial |
| Cellulose | Hydrophilic<br>Solvent resistance | Biomaterial<br>Catalyst matrix |
| Silk | Hydrophilic<br>Biocompatibility | Biomaterial<br>Cosmetic |
| γ-Poly(glutamic acid) | Hydrophilic<br>Biocompatibility | Biomaterial<br>Cosmetic |
| Polyurethane | Flexibility<br>Absorbability | Acoustic material<br>Cosmetic |

Among various polymers, poly(vinyl alcohol) (PVA) with hydroxyl groups is an outstanding biomaterial (Figure 7). Due to it excellent properties such as hydrophilic property, nontoxicity, proven mechanical strength and anabolic effect on bone formation, PVA material is often used in a variety of bio-related fields, such as tissue engineering, wound dressing and cell culture [75,76]. Thereofore, the PVA-based monolith is expected to be a potential functional material on the basis of its excellent properties.

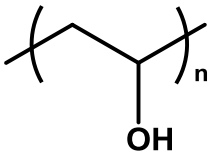


**Figure 7.** Chemical structure of PVA

With the background described above, the present thesis consists of four chapters including the following topics concerning the fabrication of PVA-based monoliths via TINIPS method and their applications.

In Chapter 1, the PVA monoliths with uniform interconnected porous structures and large specific surface area in a single piece are prepared by TINIPS for the first time. The morphology of fabricated monolith is observed by SEM, the surface area is determined by the BET method, the pore size distribution is obtained through the NLDFT method, and the microcrystallinity is investigated via XRD. The pore and skeleton sizes of the monolith are controlled by varying the fabrication parameters such as molecular weight, polymer concentration and cooling temperature. The PVA monolith is successfully crosslinked with glutaraldehyde (GA) and become water-insoluble. The crosslinking density can be easily tuned by changing the concentration of GA, and the crosslinking time. The PVA monolith possessing relatively large surface area and mesoporous structures can offer various bio-related applications.

In Chapter 2, a stimuli-responsive PVA/sodium alginate (SA) blend monolith is fabricated by TINIPS method. The blend monolith with stimuli-responsive properties is prepared by selection of appropriate phase separation conditions for the first time. The blend monoliths with different ratios of PVA and SA are fabricated. The surface area is measured by the BET method and the pore size distribution is investigated via the

NLDFT method. The interaction between PVA and SA is analyzed by FT-IR analysis. The stimuli-responsive properties of the obtained monolith are also discussed.

In Chapter 3, a PVA/hydroxyapatite composite monolithic scaffold is designed and prepared. The PVA monolith is prepared by TINIPS as porous matrix; the hydroxyapatite (HAp) mineralization on the PVA monolith is realized by an alternative soaking method. The morphology of HAp mineralized on the PVA monolith is observed by SEM. The characteristics of the composite monolith are investigated by XRD, EDX, and FR-IR analysis. The effect of soaking time and reaction cycle on the formation of HAp is also discussed. The obtained composite monolith is a candidate for the application of tissue engineering.

In Chapter 4, an acetoacetylated PVA monolith with acetoacetyl groups is fabricated via TINIPS method. By appropriate seletion of solvent/non-solvent and precisely tuning of the solvent composition, the monolith is successfully obtained. The obtained monolith is selected as a support for enzyme immobilization. It is modified with branched polyethylenimine (PEI), a common used polycartion with amine-rich structure, and subsequently with glutaraldehyde (GA), a famous reagent for enzyme immobilization. The modified monolith is finally used as a support for the enzyme immobilization.

## Reference


1. Mould DL, Synge RLM, *Analyst* 1952, **77**, 964.
2. Kubín M, Špaček P, Chromeček R, Czechosl C, *Chem. Comm.* 1967, **32**, 3881.
3. Ross WD, Jefferson RT, *J. Chromatogr. Sci.* 1970, **8**, 386.
4. Schnecko H, Bieber O, *Chromatographia* 1971, **4**, 109.

5. Hansen LC, Sievers RE, *J. Chromatogr.* 1974, **99**, 123.
6. Hjerten S, Liao JL, Zhang R, *J. Chromatogr.* 1989, **473**, 273.
7. Hjertén S, Mohammad J, Nakazato K, *J. Chromatogr.* 1993, **646**, 121.
8. Tennikova TB, Svec F, Belenkii BG, *J. Liquid Chromatogr.* 1990, **13**, 63.
9. Tennikova TB, Bleha M, Svec F, Almazova TV, Belenkii BG, *J. Chromatogr.* 1991, **555**, 97.
10. Svec F, Fréchet JMJ, *Anal. Chem.* 1992, **54**, 820.
11. Minakuchi H, Nakanishi K, Soga N, Ishizuka N, Tanaka N, *Anal. Chem.* 1996, **68**, 3498.
12. Tanaka N, Ishizuka N, Hosoya K, Kimata K, Minakuchi H, Nakanishi K, Soga N, *Kuromatogurafi* 1993, **14**, 50.
13. Fields SM, *Anal. Chem.* 1996, **68**, 2709.
14. Gritti F, Guiochon G, *J. Chromatogr. A* 2012, **1228**, 2.
15. Lau CH, Li P, Li F, Chung TS, Paul DR, *Prog. Polym. Sci.* 2012, http://dx.doi.org/10.1016/j.progpolymsci.2012.09.006.
16. Ambashta RD, Sillanpää MET, *J. Environ. Radioact.* 2012, **105**, 76.
17. Maya F, Svec F, J. Chromatogr. A 2013, **22**, 32.
18. Tswett MS, Varshav TP, Estestvoistpyt O, *Otd. Biol.* 1903, publ. 1905, **14**, 20.
19. Kennedy RT, Jorgenson JW, *Anal. Chem.* 1989, **61**, 1128.
20. Josic D, Buchacher A, Jungbauer A, *J. Chromatogr B* 2001, **752**, 191.
21. Jungbauer A, *J. Chromatogr. A* 2005, **1065**, 3.
22. Lubbad S, Mayr B, Huber CG, Buchmeiser MR, *J. Chromatogr. A* 2002, **959**, 121.
23. Mayr B, Tessadri R, Post E, Buchmeiser MR, *Anal. Chem.* 2001, **73**, 4071.
24. Peters EC, Svec F, Frèchet JMJ, *Adv. Mater.* 1999, **11**, 1169.

25. Tanaka N, Kobayashi H, Nakanishi K, Minakuchi H, Ishizuka N, *Anal. Chem.* 2001, **73**, 420A

26. Fu H, Huang X, Jin W, Zou HF, Curr. Opin. *Biotechnol.* 2003, **14**, 96.

27. Bedair M, Rassi Z, *Electrophoresis* 2004, **25**, 4110.

28. Xie C, Fu H, Hu J, Zou H, *Electrophoresis* 2004, **25**, 4095.

29. K. Mistry, N. Grinberg, *J. Liquid Chromatogr.* 2005, **28**, 1055.

30. Bakry R, Bonn GK, Mair D, Svec F, *Anal. Chem.* 2007, **79**, 486.

31. Svec F, *J. Chromatogr. B* 2006, **841**, 52.

32. Josic D, Buchacher A, *J. Biochem. Biophys. Methods* 2001, **49**, 153.

33. Krenkova J, Foret F, *Electrophoresis* 2004, **25**, 3550.

34. Svec F, *Electrophoresis* 2006, **27**, 947.

35. Weichelt F, Frerich B, Lenz S, Tiede S, Buchmeiser MR, *Macromol. Rapid Commun.* 2010, **31**, 1540.

36. Rohr T, Yu C, Davey MH, Svec F, Frechet JMJ, *Electrophoresis* 2001, **22**, 3959.

37. Peters EC, Svec F, Frechet JMJ, *Adv. Mater.* 1997, **9**, 630.

38. Yu C, Mutlu S, Selvaganapathy P, Mastrangelo CH, Svec F, Frechet JMJ, *Anal. Chem.* 2003, **75**, 1958.

39. Luo Q, Mutlu S, Gianchandani YB, Svec F, Frechet JMJ, *Electrophoresis* 2003, **24**, 3694.

40. Bartolini M, Cavrini V, Andrisano V, *J. Chromatogr. A* 2007, **1144**, 102.

41. Delattre C, Michaud P, Vijayalakshmi MA, *J. Chromatogr. B* 2008, **861**, 203.

42. Kawakami K, Abe D, Urakawa T, Kawashima A, Oda Y, Takahashi R, Sakai S, *J. Sep.Sci.* 2007, **30**, 3077.

43. Mosbach K, Immobilized Enzymes, Academic Press, New York 1976.

44. Mosbach K, Immobilized Enzymes, Academic Press, New York 1987.

45. Siouffi AM, *J. Chromatogr. A* 2003, **1000**, 801.

46. Ghanem A, Ikegami T, *J. Sep. Sci.* 2011, **34**, 1945.

47. Ishizuka N, Minakuchi H, Nakanishi K, Soga N, Nagayama H, Hosoya K, Tanaka N, *Anal. Chem.* 2000, **72**, 1275.

48. Tanaka N, Nagayama H, Kobayashi H, Ikegami T, Hosoya K, Ishizuka N, Minakuchi H, Nakanishi K, Cabrera K, Lubda D, *J. High Resol. Chromatogr.* 2000, **23**, 111.

49. Minakuchi H, Nakanishi K, Soga N, Ishizuka N, Tanaka N, *J. Chromatogr. A* 1998, **797**, 121.

50. Nakanishi K, Minakuchi H, Soga N, Tanaka N, *J. Sol-Gel Sci. Technol.* 1997, **8**, 547.

51. Nunez O, Ikegami T, Kajiwara W, Miyamoto K, Horie K, Nataka N, *J. Chromotogr. A* 2007, **1156**, 35.

52. Siouffi AM, *J. Chromatogr. A* 2003, **1000**, 801.

53. Nunez O, Nakanishi K, Tanaka N, *J. Chromatogr. A* 2008, **1191**, 231.

54. Shi ZG, Feng YQ, Xu L, Zhang M, Da SL, *Talanta* 2004, **63**, 593.

55. Svec F, *J. Chromatogr. A* 2010, **1217**, 902.

56. Zuo Z, Guo Y, Li Y, Lv J, Liu H, Xu J, Li Y, *Macromol. Rapid Commun.* 2009**, 30**, 1940.

57. Svec F, Fréchet JMJ, *Macromolecules* 1995, **28**, 7580.

58. Viklund C, Svec F. Fréchet JMJ, Irgum K, *Chem. Mater.* 1996, **8**, 744.

59. Peters EC, Svec F, Fréchet JMJ, Viklund C, Irgum K, *Macromolecules* 1999, **32**, 6377.

60. Viklund C, Pontén E, Glad B, Irgum K, Hörsted P, Svec F, *Chem. Mater.* 1997, **9**, 463.

61. Viklund C, Irgum K, *Macromolecules* 2000, **33**, 2539.

62. Gu B, Li Y, Lee ML, *Anal. Chem.* 2007, ***79***, 5848.

63. Li Y, Gu B, Dennis TH, Lee ML, *J. Chromatogr. A* 2009, **1216**, 5525.

64. Grasselli M, Smolko E, Hargittai P, Sárfrány Á, *Nucl. Instr. Meth. Phys. Res. B* 2001, **185**, 254.

65. Buchmeiser MR, *Macromol. Rapid Commun.* 2001, **22**, 1081.

66. Kanamori K, Nakanishi K, Hanada T, *Adv. Mater.* 2006, **18**, 2407.

67. Barby D, Haq Z, *Europ. Pat.* 1982, Nr. 0060138.

68. Small PW, Sherrington DC, *J. Chem. Soc., Chem. Commun.* 1989, 1589.

69. Hainey P, Huxham IM, Rowatt B, Sherrington DC, Tetley L, *Macromolecules* 1991, **24**, 117.

70. Tsujioka N, Hira N, Aoki S, Tanaka N, Hosoya K, *Macromolecules* 2005, **38**, 9901.

71. Nguyen AM, Irgum K, *Chem. Mater.* 2006, **18**, 6308.

72. Okada K, Nandi M, Maruyama J, Oka T, Tsujimoto T, Kondoh K, Uyama H, *Chem. Commun.* 2011, **47**, 7422.

73. Nandi M, Okada K, Uyama H, *Funct. Mater. Lett.* 2011, **4**, 407.

74. Xin Y, Fujimoto T, Uyama H, *Polymer* 2012, **53**, 2847.

# Chapter 1

# Fabrication of Poly(vinyl alcohol) Monolith via Thermally Impacted Non-Solvent Induced Phase Separation

## 1.1 Introduction

In general, “monolith" means "one piece". In the field of chromatography, it is used in contrast to particulate stationary phase [1, 2]. In the last two decades, considerable attention has been paid on the monoliths due to their excellent permeability, fast mass transfer performance, high stability and ease of chemical modification [3-5]. On the basis of these favorable properties, monolithic materials can be widely used for various fields [6-15].

Polymer-based monolith, one main type of monolith, have been of increasingly greater interest not merely for their predominant pH stability, non-specific interaction, and biocompatibility, but also owing to their specific pore properties and easy functionalization [16-21].

Among a variety of fabrication techniques, a novel approach based on phase separation method is developed in the author’s laboratory. There are two main types of this technique, TIPS method and NIPS method respectively. By utilizing the TIPS method, PMMA and PAN monoliths have been fabricated successfully; while through the NIPS method, PC monolith has been prepared [22-24]. A great advantage of this method is to use polymer itself instead of the monomers. Besides, the shape of the monoliths can also be easily modified by altering the shape of the vessel.

This chapter mainly addresses the fabrication of PVA monolith via TINIPS method. This method is developed based on the NIPS method, but moreover introduces a

thermal factor. Traditionally, the NIPS method is adopted to fabricate porous membrane in industrial fields [25, 26]. Compared to other traditional fabrication techniques which almost use monomer as the starting material, TINIPS method is a remarkably simple and clean process that involves the addition of non-solvent to the polymer solution at high temperature and the subsequent cooling of the mixed solution containing a polymer, a solvent and a non-solvent. Adding of the non-solvent makes the initial solution become unstable and it separates into polymer-rich phase and polymer-lean phase. In the cooling process, the phase separation takes place. The polymer chains in the polymer-rich phase aggregate and develop into a continuous matrix; while the polymer-lean phase mainly containing the solvent mixture flow through the matrix leading to porous channels within the monolith. When the phase separation of the polymer is completed, the monolithic column is formed (Figure 1-1). Moreover, this method is template-free; thus it enables the convenient fabrication of functional monoliths to satisfy a great variety of demand for different shapes.

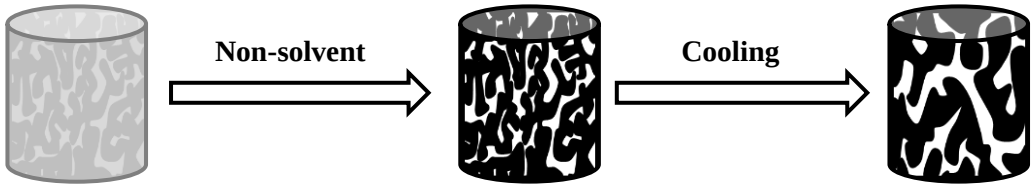


**Figure 1-1.** Phase separation during the TINIPS process

PVA monolith is a potential functional material due to its excellent properties such as biocompatibility, nontoxicity, proven mechanical strength and anabolic effect on bone formation [27-30]. In this chapter, the PVA monolith with continuous porous structure is fabricated successfully via TINIPS method for the first time. The gross

shape and inside structure of the PVA monolith can be controlled precisely through adjusting the fabrication parameters.

## 1.2 Experimental

### Materials

PVA powders with hydrolysis ratio of 98 % and different molecular weights were purchased from Wako Pure Chemical Industries, Ltd. and Sigma-Aldrich Co. Glutaraldehyde (GA) solution (50 wt%) was obtained from Sigma-Aldrich Co. Hydrochloric acid (1 mol/L) was purchased from Wako Pure Chemical Industries, Ltd. Other reagents and solvents were used as received.

### Measurements

The microstructure of PVA monolith was observed by a scanning electron microscope (SEM, S-3000N, Hitachi Ltd., Japan) at 15 kV. Before observation, the sample was cut with a scalpel, and was coated with a thin layer of gold by an ion sputter apparatus (E-1010 Ion Sputter, Hitachi Ltd., Japan). Specific surface area of the samples was measured by a nitrogen adsorption apparatus using Brunauer-Emmett-Teller (BET) method (NOVA 4200e, Quantachrome instruments, USA). Fourier transform infrared (FT-IR) absorption spectra were recorded by Nicolet iS 5 (Thermo Scientific, Japan). X-ray diffraction (XRD) patterns were obtained by an XRD-6100 (Sigmadzu Corp., Japan) at a scanning rate of 4.0 deg/min from 10 to 70 deg (2θ). The measurement was performed under the conditions of 40 kV and 30mA using Cu-Kα radiation (λ=1.5418 Å).

**Preparation of PVA monolith**

PVA powder was firstly dissolved into distilled water at 95 ºC for about 3h with constant stirring at 400 rpm to form a homogeneous aqueous PVA solution. The solution was cooled to 55 ºC, and then acetone (non-solvent) was added into it dropwise to avoid the formation of precipitates. Afterward the mixture was kept at 20 ºC for 24h, at which period the phase separation took place to form a white monolithic material. The solvent in the monolith was replaced with acetone by immersion of the monolith into 60 mL of acetone for 12 h under gentle shaking. The solvent replacement was repeated three times and the monolith was finally dried in vacuo.

**Crosslinking of PVA monolith by GA**

The monolith (210 mg) was immersed into 15mL of the GA solution with 0.3 mL of 1 M HCl as catalyst for different hours. The monolith was washed with distilled water until the washed water became neutral, and dried in vacuo for 12 h.

**Determination of swelling ratio of PVA monolith**

The PVA monolith (about 210 mg) was immersed in 20 mL of water at room temperature. The weight change was measured every 5 min until the weight became almost constant. The experimental was carried out three times. The swelling ratio was calculated as follows [31]:

$$swelling\ ratio\ (\%) = (W_b - W_e) / W_e \times 100$$

where $W_e$ and $W_b$ were the weights before and after the immersion in water, respectively.

## 1.3 Results and Discussion

### Fabrication and Characterizations of PVA monolith

PVA monolith is firstly fabricated from the mixture containing PVA, water and acetone. The fabrication conditions are as follows: the cooling temperature of 20 °C, the PVA concentration of 60 mg/mL, the PVA molecular weight of $8.8x10^4$, and the water/acetone mixed ratio of 4/3. The inside morphology of the PVA monolith is observed by SEM, which shows the three-dimensional open pore structures of the monolith (Figure 1-2). The average pore and skeleton sizes of the PVA monolith are 2.0 μm and 1.1 μm, respectively.

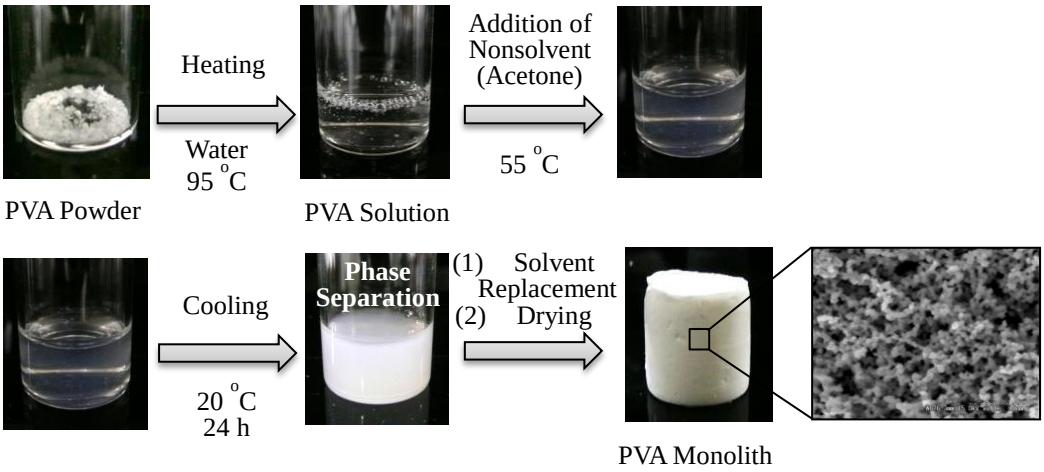


**Figure 1-2.** Fabrication processes of PVA monolith

The adsorption-desorption isotherm of the PVA monolith is shown in Figure 1-3 (A). The isotherm is ascribed to type IV demonstrating that there exist mesopores in the monolith. The isotherm at the beginning is of monolayer adsorption, followed by multilayer adsorption, and the hysteresis in the multilayer range is associated with capillary condensation in mesopore structures. The hysteresis loop in the $P/P_0$ range

from 0.7 to 1.0 is of type H1 that means the PVA monolith contains cylindrical pores with narrow distributions of pore size [32, 33]. The BET surface area is 110 $m^2/g$ and the pore size distribution (PSD) plot for the sample obtained by using the non-local density functional theory (NLDFT) method reveals relatively uniform mesopores with pore diameter of 7-25 nm (Figure 1-3 (B)). These results indicate that the PVA monolith is a mesoporous material with large surface area.

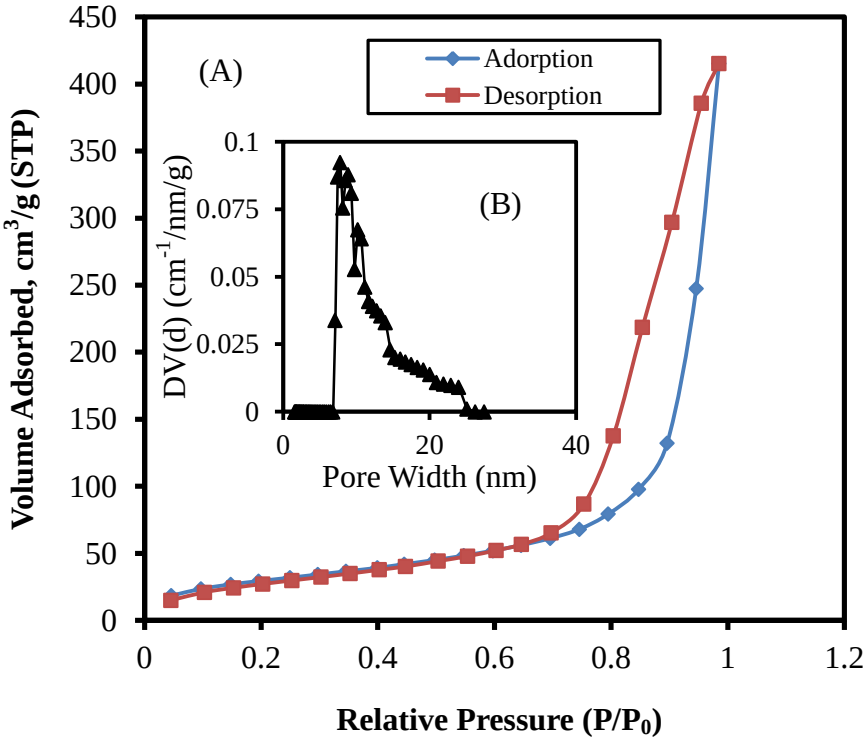


**Figure 1-3.** Nitrogen adsorption-desorption isotherms of PVA monolith

The crystalline structure of the monolith is examined by the wide angle XRD (Figure 1-4). The relatively sharp and intense peak is observed at 2θ=19.5 ° for the monolith, which is almost the same as that of the PVA powder. The microcrystallites of the PVA powder are reported to be formed by the aggregation of hydrogen bonds between the hydroxyl groups [34, 35]. The similar results of XRD for the monolith and

powder of PVA strongly suggest that the microcrystallites of the PVA monolith are also configurated via hydrogen bonds.

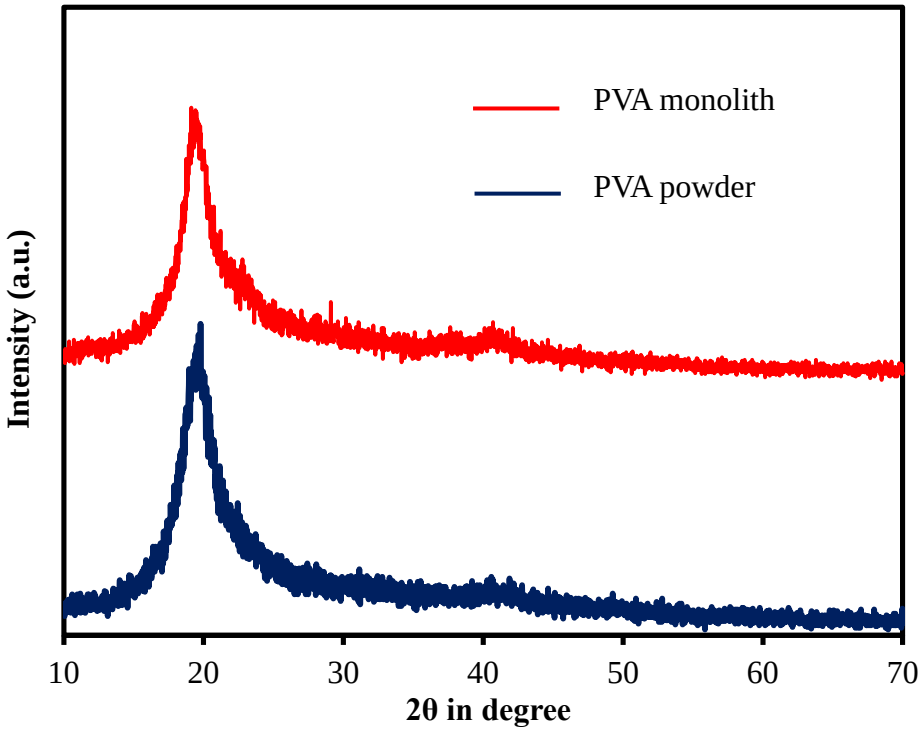


**Figure 1-4.** X-ray diffraction pattern of PVA powder and PVA monolith

**Morphological control of PVA monolith**

The mixed ratio of water and acetone is examined under the conditions of the cooling temperature of 20 °C, the PVA concentration of 60 mg/mL, and the PVA molecular weight of $8.8 \times 10^4$. As described above, the water/acetone mixed ratio of 4/3 affords the monolith of the uniform shape. On the other hand, the phase separation does not take place in the mixed ratio of 2/1, resulting in no formation of the monolith. The PVA powder is not completely solubilized in the mixed ratio of 1/1. These results indicate that the mixed ratio of 4/3 is a crucial factor for the fabrication of the PVA monolith.

Figure 1-5 shows the SEM photographs of the PVA monolith fabricated with cooling temperatures of –196, –20, and 20 ºC under the conditions of the PVA concentration of 60 mg/mL, the PVA molecular weight of $8.8x10^4$, and the water/acetone mixed ratio of 4/3. The average skeleton and pore sizes increase with increasing the cooling temperature (Figure 1-6 and Table 1-1). It could be explained that at higher temperature, PVA molecules can move more freely and have long enough time to coagulate to form the monolith with larger skeleton and pore sizes, whereas at lower temperature, the movement of PVA molecules is limited and the phase separation takes place faster to reduce skeleton and pore sizes. When the cooling temperature is –196 ºC, the mixture is frozen instantaneously, resulting in the smallest skeleton and pore sizes.

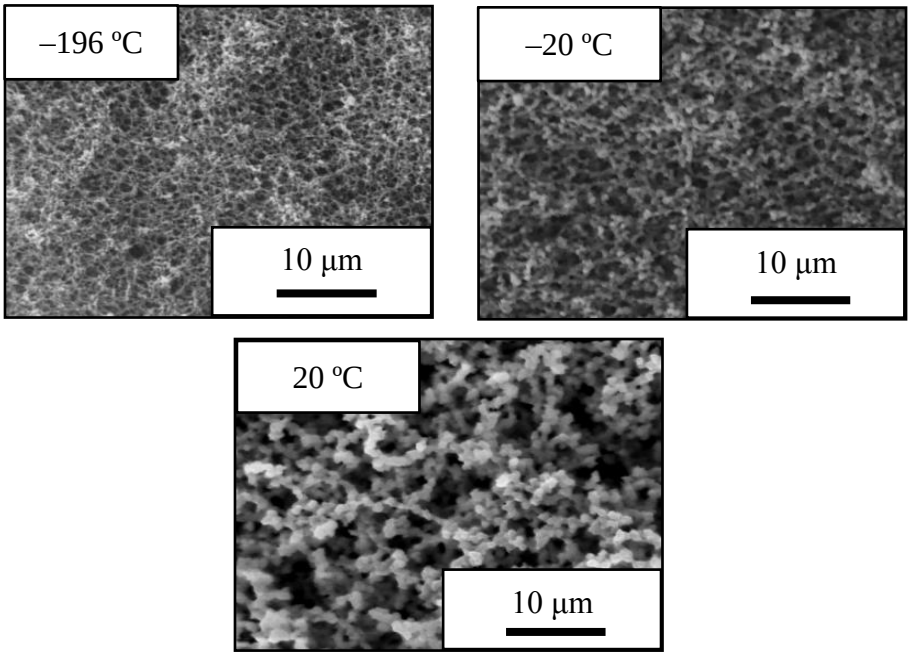


**Figure 1-5.** SEM photography of microstructures of PVA monolith fabricated at different cooling temperatures

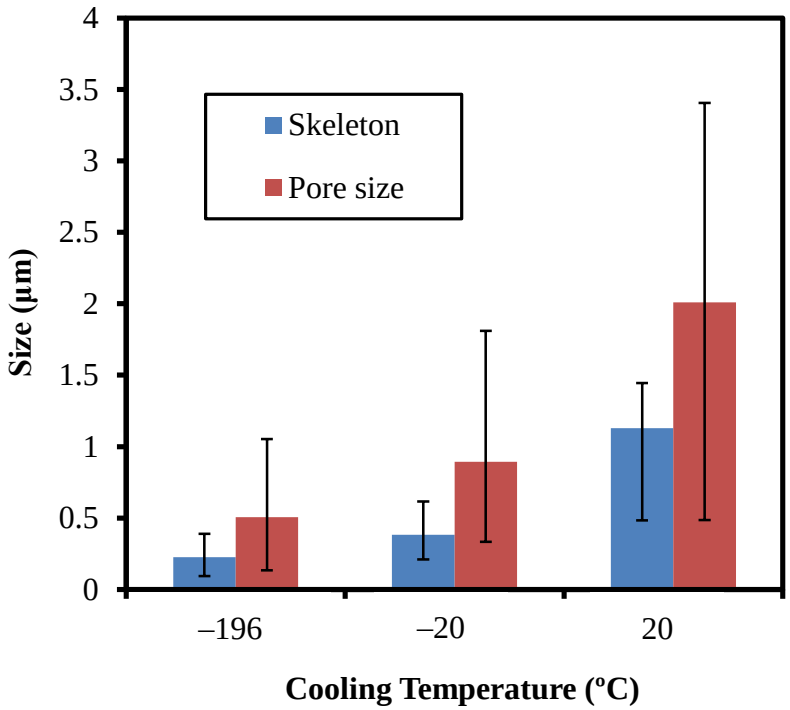


**Figure 1-6.** Effect of cooling temperatures on average pore and skeleton sizes

**Table 1-1.** Effect of cooling temperatures on average pore and skeleton sizes

| **Cooling temperature (°C)** | **–196** | **–20** | **20** |
|---|---|---|---|
| **Pore size (µm)** | 0.51 | 0.89 | 2.01 |
| **Skeleton (µm)** | 0.23 | 0.38 | 1.13 |

Next, the effect of the PVA concentration on the morphology of the monolith has been examined. Figure 1-7 shows SEM photographs of the PVA monolith fabricated with different PVA concentrations under the conditions of the cooling temperature of 20

ºC, the PVA molecular weight of $8.8 \times 10^4$, and the water/acetone mixed ratio of 4/3. In all the cases examined, relatively uniform skeleton is formed. The skeleton and pore sizes decrease as a function of the PVA concentration in the range of 40-80 mg/mL (Figure 1-8 and Table 1-2). These data strongly suggest that the morphology control is easily made by changing the cooling temperature and PVA concentration. With the increase of the viscosity of the polymer solution, the higher degree of entanglement results in the slower dynamics of the phase separation. Therefore, the increase of the PVA concentration leads to the decrease of the skeleton and pore sizes in the fabrication of the PVA monolith.

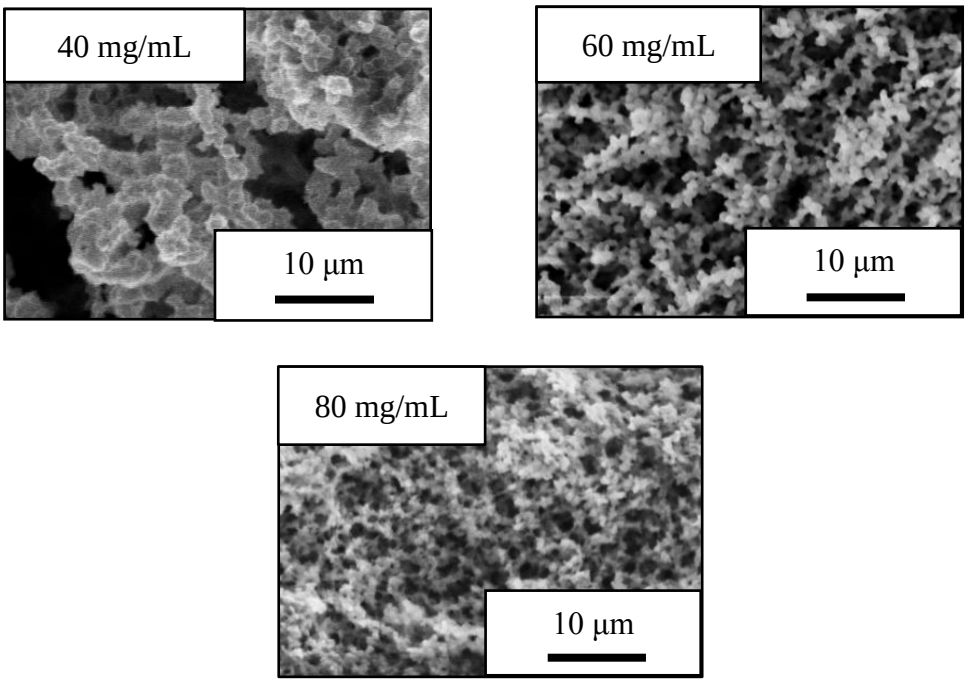


**Figure 1-7.** SEM photography of microstructures of PVA monolith fabricated from different concentrations of PVA

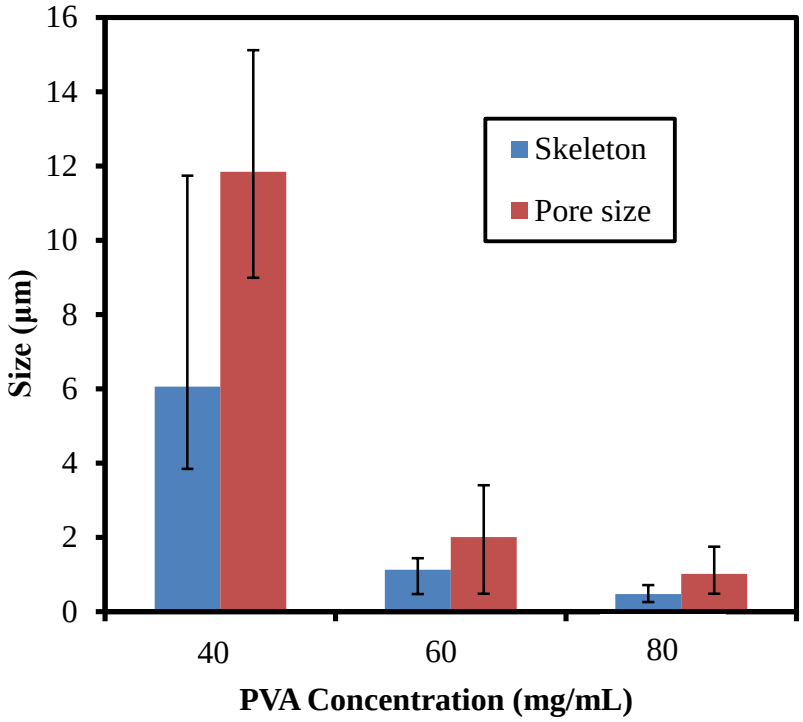


**Figure 1-8.** Effect of PVA concentration on average pore and skeleton sizes

**Table 1-2.** Effect of PVA concentration on average pore and skeleton sizes

| **Concentration (mg/mL)** | **40** | **60** | **80** |
|---|---|---|---|
| **Pore size (µm)** | 6.06 | 1.13 | 0.48 |
| **Skeleton (µm)** | 11.85 | 2.01 | 1.02 |

In the above experiments, the monolith is fabricated by using PVA with molecular weight of $8.8 \times 10^4$. Additionally, PVAs with different molecular weights of $1.8 \times 10^4$ and $1.7 \times 10^5$ are used to examine the effect of the PVA molecular weight on the morphology

of the monolith under the conditions of the cooling temperature of 20 ºC, the PVA concentration of 60 mg/mL, and the water/acetone mixed ratio of 4/3 (Figure 1-9). In all the cases examined, the monolith is formed. When the molecular weight is $1.8x10^4$, the skeleton and pore sizes are larger than those with higher molecular weight (Figure 1-10 and Table 1-3). The difference of these sizes between molecular weight of $8.8x10^4$ and $1.7x10^5$ is relatively small. These data clearly show that PVA with wide range of the molecular weight is applicable for the fabrication of the PVA monolith by the TINIPS method and the molecular weight affects the morphology of the PVA monolith. The morphology difference may be due to the mobility of the polymer chain in the present system; the domain formation in the phase separation is strongly affected by the viscosity of the polymer solution of PVA, dependent on the molecular weight.

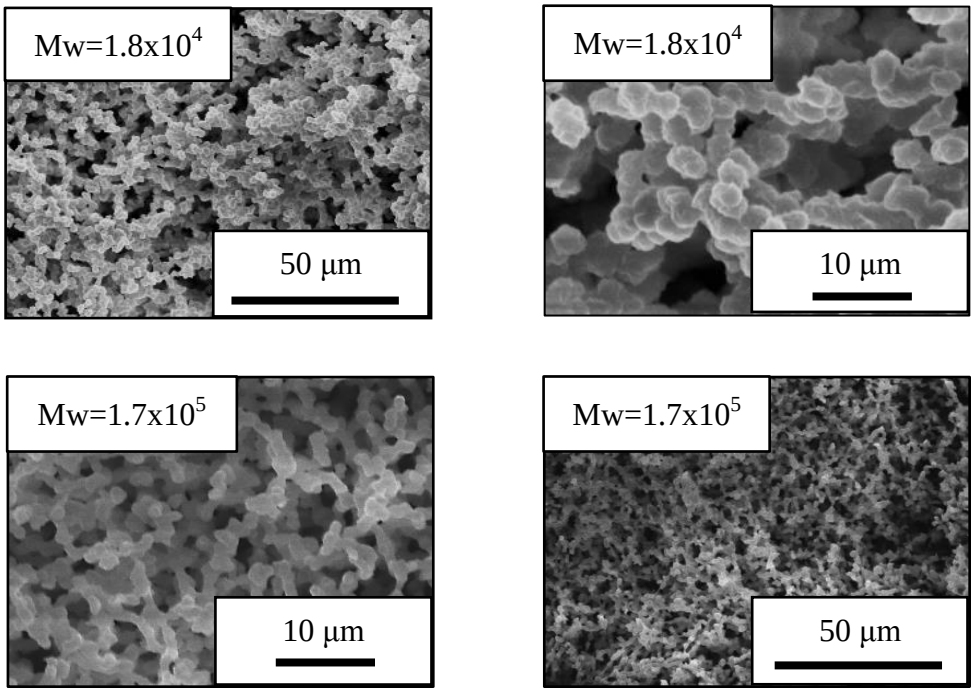


**Figure 1-9.** SEM photography of microstructures of PVA monolith fabricated with different molecular weight of PVA

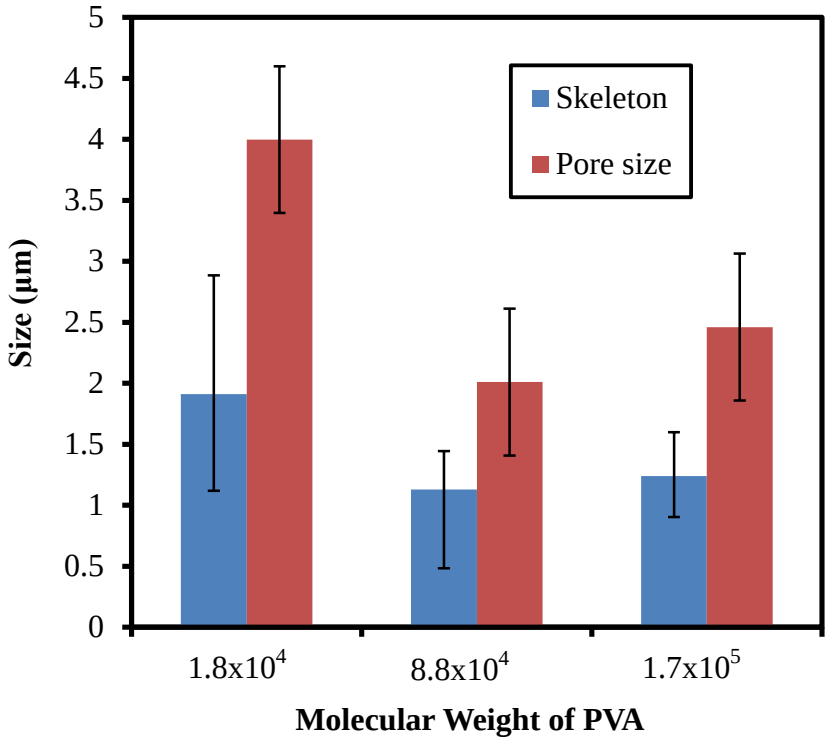


**Figure 1-10.** Effect of molecular weight on average pore and skeleton sizes

**Table 1-3.** Effect of molecular weight on average pore and skeleton sizes

| **Molecular of PVA** | **1.3 ×10$^4$** | **8.8×10$^4$** | **1.7 ×10$^5$** |
|---|---|---|---|
| **Pore size (µm)** | 1.91 | 1.13 | 1.24 |
| **Skeleton (µm)** | 4.00 | 2.01 | 2.46 |

**Crosslinking of PVA monolith**

Glutaraldehyde (GA) is known to be an effective crosslinking agent for PVA [36]. In this study, GA is selected to crosslink the PVA monolith. The crosslinking is performed by the immersion of the monolith in the GA solution with the concentrations

of 6.25, 12.5, and 25 wt% for 6, 12 or 24 h in the presence of a small amount of HCl as catalyst. In all the cases, the crosslinking smoothly takes place to form the water-insoluble monolith. The crosslinking is confirmed by FT-IR (Figure 1-11). In the FT-IR spectrum of the product after the crosslinking, a strong peak at 1720 $cm^{-1}$ ascribed to carbonyl group of aldehyde and two peaks at 2850 and 2750 $cm^{-1}$ due to C-H stretching newly appear [37, 38]. Furthermore, the intensity of the broad peak around 3300 $cm^{-1}$ due to O-H stretching of PVA relatively decreases in comparison with that of PVA. These results suggest that the hydroxyl group of PVA is reacted with GA to form the acetal bridge, leading to the crosslinking of the PVA chain.

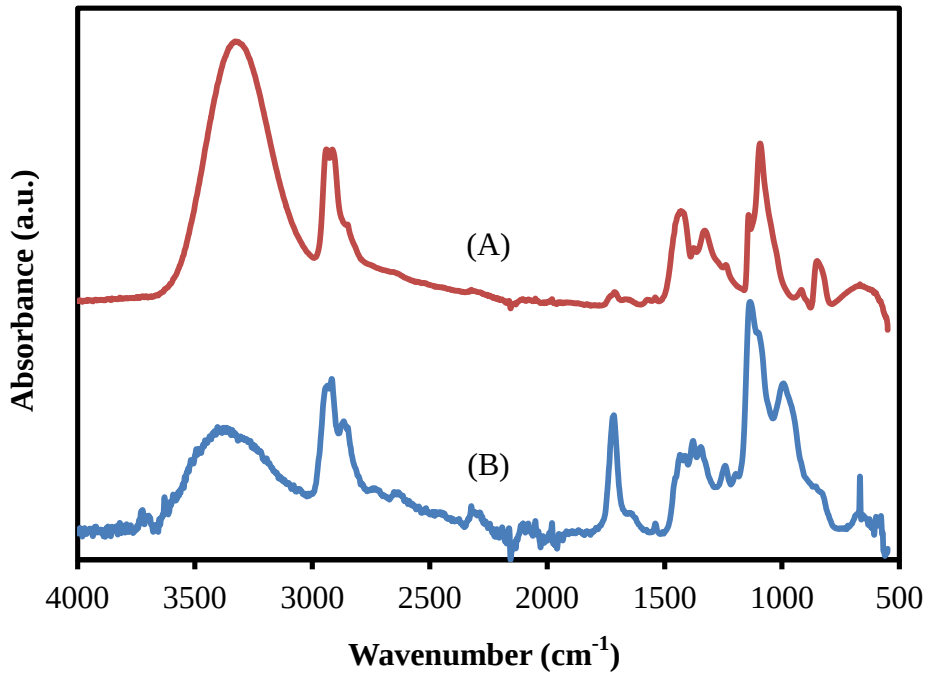


**Figure 1-11.** FT-IR Specta of PVA monolith of (A) before and (B) after the crosslinking with GA

The degree of the crosslinking is regarded as swelling ratio of the crosslinked monolith. In most cases, the swelling equilibrium reaches within 1 h. Figure 1-12 (A) shows the effect of the GA concentration on the swelling ratio of the sample crosslinked for 24 h. As the concentration increases, the swelling ratio decreases, suggesting that the concentration of GA solution plays an important role in the swelling ratio. The crosslinking period also affects the swelling ratio (Figure 1-12 (B)). In case of the GA concentration of 25 wt %, the swelling ratio decreases as a function of the reaction time. These results suggest that the crosslinking density and swelling ratio of the PVA monolith can be easily tuned by changing the crosslinking conditions.

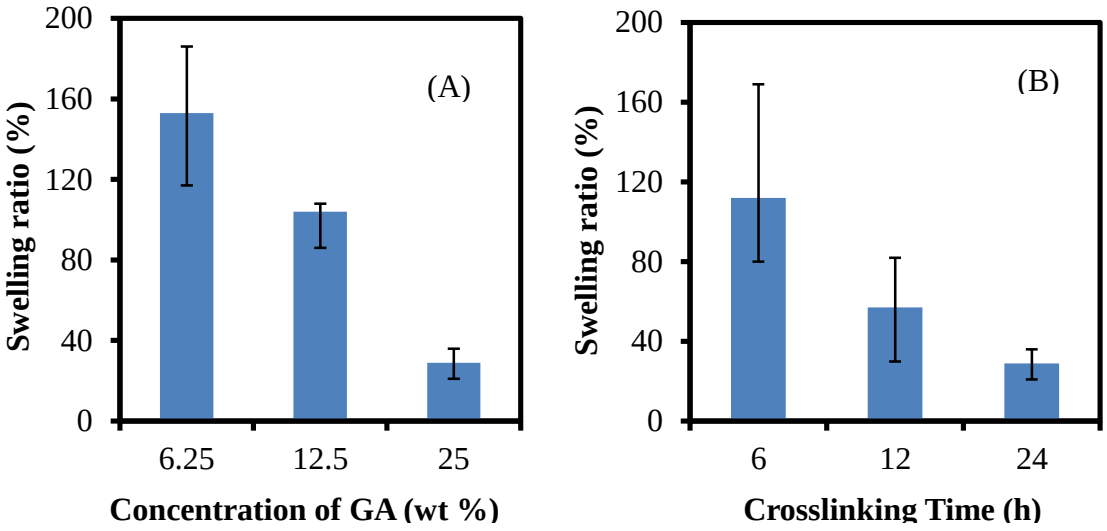


**Figure 1-12.** Swelling behavior of PVA monolith with (A) different concentration of GA and (B) different crosslinking time

## 1.4 Conclusion

A new methodology of monolith via thermally impacted non-solvent induced phase separation (TINIPS) has been developed to produce a hydrophilic monolith. When the water/acetone mixed ratio is 4/3, the PVA monolith with the uniform structure and large specific surface area is formed. By changing the concentration and molecular weight of PVA as well as the cooling temperature, the skeleton and pore sizes can be easily controlled. Furthermore, the monolith is converted into the water-insoluble one by the crosslinking with GA. The swelling ratio depends on the GA concentration and the crosslinking time.

So far, most of the reported monoliths are composed of hydrophobic polymers. In this study, a monolith of PVA with hydrophilic and biocompatible properties is conveniently fabricated by TINIPS. The synthetic process of monoliths from a polymer itself as precursor by using the phase separation techniques (TIPS, NIPS and TINIPS) provides their new applications in various fields. Further studies on the application of the crosslinked PVA monolith for bioseparation/purification are under way in our laboratory.

## 1.5 Reference


1. Scheibitz B, Prager A, Buchmeiser MR, *Macromolecules* 2009, **42**, 3493.
2. Beckert S, Stallmach F, Bandari R, Buchmeiser MR, *Macromolecules* 2010, **43**, 9441.
3. Rose M, Klein N, Senkovska I, Schrage C, Wollmann P, Böhlmann W, Böhringer B, Fichtner S, Kaskel S, *J. Mater. Chem.* 2011, **21**, 711.
4. Urban J, Svec F, Fréchet JMJ, *Biotechnol. Bioeng*. 2012, **109**, 371.
5. Walsh Z, Levkin PA, Abele S, Scarmagnani S, Heger D, Klán P, Diamond D, Paull

B, Svec F, Macka M, *J. Chromatogr., A* 2011, **1218**, 2954.

6. Nordborg A, Hilder EF, Haddad PR, *Annu. Rev. Anal. Chem.* 2011, **4**, 197.
7. Peters EC, Petro M, Svec F, Fréchet JMJ, *Anal. Chem.* 1997, **69**, 3646.
8. Eeltink S, Herrero-Martinez JM, Rozing GP, Schoenmakers PJ, Kok WT, *Anal. Chem.* 2005, **77**, 7342.
9. Tao S, Wang Y, An Y, *J. Mater. Chem.* 2011, **21**, 11901.
10. Liu Y, Ren L, Liu Z, *Chem. Commun.* 2011, **47**, 5067.
11. Izquierdo-Barba I, Vallet-Regí M, Kupferschmidt N, Terasaki O, Schmidtchen A, Malmsten M, *Biomaterials* 2009, **30**, 5729.
12. Worsley MA, Stadermann M, Wang YM, Satcher Jr JH, Baumann TF, *Chem. Commun.* 2010, **46**, 9253.
13. Aguado S, Canivet J, Farrusseng D, *J. Mater. Chem.*2011, **21**, 7582.
14. Bourret GR, Goulet PJG, Lennox RB, *Chem. Mater.*2011, **23**, 4954.
15. Sachse A, Hulea V, Finiels A, Coq B, Fajula F, Galarneau A, *J. Catal*. 2012, **287**, 62.
16. Li Y, Tolley HD, Lee ML, *Anal. Chem.* 2009, **81**, 9416.
17. Chen X, Tolley HD, Lee ML, *J. Chromatogr. A* 2010, **1217**, 3844.
18. Satterfield BC, Stern S, Caplan MR, Hukari KW, West JAA, *Anal. Chem.* 2007, **79**, 6230.
19. Sáfrány Á, Beiler B, László K, Svec F, *Polymer* 2005, **46**, 2862.
20. Sinner F, Buchmeiser MR, *Macromolecules* 2000, **22**, 5777.
21. Sudheendran M, Buchmeiser MR, *Macromolecules* 2010, **43**, 9601.
22. Okada K, Nandi M, Maruyama J, Oka T, Tsujimoto T, Kondoh K, Uyama H, *Chem. Commun*. 2001, **47**, 7422.
23. Nandi M, Okada K, Uyama H, *Funct. Mater Lett*. 2011, **4**, 407.

24. Xin Y, Fujimoto T, Uyama H, *Polymer* 2012, **53**, 2847.

25. Yen C, He H, Lee LJ, Ho WSW, *J. Membrane Sci*. 2009, **343**, 180.

26. Susanto H, Ulbricht M, *J. Membrane Sci*. 2009, **327**, 125.

27. Hassan CM, Peppas NA, *Adv. Polym. Sci*. 2000, **153**, 37.

28. Zhu H, Li Y, Qiu R, Shi L, Wu W, Zhou S, *Biomaterials* 2012, **33**, 3058.

29. Lee H, Mensire R, Cohen RE, Rubner MF, *Macromolecules* 2012, **45**, 347.

30. Zhou Y, Yang D, Chen X, Xu Q, Lu F, Nie J, *Biomacromol*. 2008, **9**, 349.

31. Bai X, Ye Z, Li Y, Ma Y, *J. Appl. Polym. Sci.* 2010, **117**, 2732.

32. Sing KSW, *Pure & Appl. Chem.* **1982, 54**, 2201.

33. Coleman NJ, Hench LL, *Ceram. Int.* 2000, **26**, 171.

34. Bunn CW, *Nature* 1948, **161**, 929.

35. Otsuka E, Sugiyama M, Suzuki A, *Polym. Bull.* 2011, **67**, 1215.

36. Du H, Zhang J, *Soft Matter* 2010, **6**, 3370.

37. Mansur HS, Oréfice RL, Mansur AAP, *Polymer* 2004, **45**, 7193.

38. Mansur HS, Sadahira CM, Souza AN, Mansur AAP, *Mater. Sci. Eng., C* 2008, **28**, 539.

# Chapter 2

# A Poly(vinyl alcohol)/Sodium Alginate Blend Monolith with Nanoscale Porous Structure

## 2.1 Introduction

Stimuli-responsive porous materials have aroused special interest not only for their pore structures, but also because they can go through the visible changes in their property to respond to environmental variation [1]. Some efforts have been made to introduce functional groups onto the pore surface of polymer monoliths, providing stimuli-responsive properties [2]. In most cases, such monoliths should be fabricated by polymerization of monomers and subsequent surface functionalization. For both processes, time-consuming procedures for precise control of the monolith structure and introduction ratio of the functional group are often involved.

In this study, the fabrication of a blend monolith of PVA and sodium alginate (SA) has been examined by TINIPS method for further functionalization of the PVA monolith. Although fabrication of monoliths consisting of more than two polymers is expected to broaden their applications in various fields, it is generally difficult to realize due to the different conditions of phase separation of the blended polymers. In many cases, only one polymer is forward subjected to the phase separation, in which others remain in the solution of the phase separation system. Previously, we successfully fabricate a blend monolith of polycarbonate and poly(3-hydroxybutyrate-co-3-hydroxyhexanoate) by precise choice of a solvent via NIPS, in which case the solvent of the phase separation is the same as that for monolith fabrication of each polymer by NIPS [3].

SA is a kind of anionic polysaccharides having a carboxylate group in the side

chain. It has excellent features such as biocompatibility, biodegradability and pH-responsive property. Based on these characteristics, SA is often used as matrix of biomaterials. The carboxylate group of SA is reported to form hydrogen bonding with the hydroxyl group of PVA [4, 5]; however, there have been few literatures focusing on the phase separation in bulk fabricated by blending of PVA and SA. Furthermore, a monolith of SA has not been fabricated up to the present. This study deals with the facile fabrication of a PVA/SA blend monolith via TINIPS on the basis of this hydrogen bonding formation. A mixed solvent of methanol and water enables the fabrication of this blend monolith, whereas the PVA monolith is formed in an aqueous acetone. To our best knowledge, SA is incorporated in polymer monoliths by selection of appropriate phase separation conditions for the first time.

## 2.2 Experimental

### Materials

Sodium alginate powders and PVA powders with a hydrolysis ratio of 98% were purchased from Wako Pure Chemical Industries, Ltd (Tokyo, Japan). All other reagents and solvents were used as received.

### Preparation of PVA/SA blend monolith

An aqueous solution of a mixture of PVA and SA (95:5 wt%) was prepared by dissolving these polymers into water at 95 °C. After cooling the polymer solution to 60 °C, methanol as non-solvent was added dropwise. Afterward, the mixture was kept at 20 °C for 36 h, during which period the phase separation occurred to form the monolithic column. The monolith was then immersed into the calcium chloride solution

for ionical crosslinking of SA. After 2 h, the monolith was washed repeatedly by acetone to remove the solvent and subsequently dried under vacuum.

**Characterizations**

Scanning electron microscopic (SEM) images were recorded on a HITACHI (Tokyo, Japan) S-3000N instrument at 15 kV. The samples were cut with a scalpel and coated with a thin layer of gold by an ion sputter apparatus (E-1010 Ion Sputter, Hitachi Ltd, Tokyo, Japan). Nitrogen adsorption/desorption isotherms were measured with a NOVA 4200e surface area & pore size analyzer (Quantachrome Instruments, Boynton Beach, FL, USA) at 25 $^{o}$C. The Brunauer Emmett Teller (BET) method was utilized to determine specific surface areas. Before the measurements, all samples were degassed at 25 $^{o}$C for 12 h under vacuum. Fourier transform infrared (FT-IR) measurements by the attenuated total reflectance (ATR) method were performed by Thermo Scientific (Yokohama, Japan) Nicolet iS5 with iD5 ATR accessory.

Porosity of the monolith samples was measured by using a gravimetric method according to the following equation:

$$\text{Porosity (\%)} = (1-V_1/V_0) \times 100$$

where $V_1$ was the volume of a certain weight of the PVA/SA blend powder and $V_0$ was the volume of the same weight of PVA/SA blend monolith.

The pH-sensitivity of PVA/SA blend monolith samples was evaluated on the basis of the swelling ratio in a solution with different pH (Fig. 5), which was determined by the following equation [6]:

$$\text{Swelling ratio (\%)} = W_b / W_e \times 100$$

where $W_e$ and $W_b$ were the weights before and after immersion, respectively.

## 2.3 Results and Discussion

The general synthetic procedure is shown as Figure 2-1. For the fabrication process, selection of non-solvent and the ratio of solvent and non-solvent are crucial factors for the formation of the blend monolith. The detailed screening of the phase separation solvent shows that a mixture of water and methanol with ratio of 2:3 is the most suitable. Intriguingly, the PVA monolith with good mechanical strength is not formed in this solvent. When the methanol ratio of the mixed solvent is more than 60 %, the precipitation takes place very quickly during the phase separation, resulting in no formation of the monolith. On the other hand, no phase separation occurs when the methanol ratio is less than 60 %. These behaviors can be rationalized as follows. After adding methanol into the polymer solution, the mixed solvent system transforms into polymer-rich phase and polymer-lean phase. As the amount of non-solvent (methanol) increases, the polymer segments in the polymer-rich phase become folded and aggregated, leading to the increase of the concentration in the polymer-rich phase. When the increasing concentration reaches to a certain degree, the phase separation takes place. In the case of smaller amount of non-solvent, the concentration of polymer-rich phase is not high enough to induce the phase separation; while for much larger amount of non-solvent, a mass of polymer segments aggregate rapidly, resulting in precipitation of the polymer in the phase separation system.

Moreover, the ionical crosslinking with $Ca^{2+}$ is an essential process for the blend monolith fabrication. Without this step, the blend monolith turns out to be drastically shrunk in the drying process and the pore structure is not maintained any more. It is probably because the hydrogen bonds formed between PVA and SA are not strong enough to keep the porous structure of the blend monolith; the crosslinked structure of SA with $Ca^{2+}$ enhances the strength of the blend monolith with preservation of the porous morphology [7].

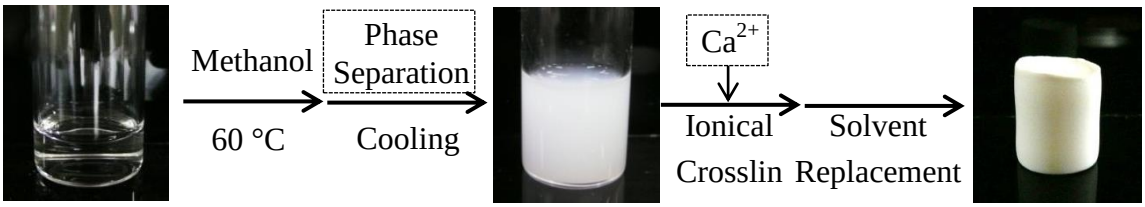


**Figure 2-1.** Fabrication process of PVA/SA blend monolith via TINIPS method

The blend monoliths with different mixed ratios of PVA/SA = 95/5, 90/10, and 85/15 (PVA/SA-1, PVA/SA-2, and PVA/SA-3, respectively) are successfully fabricated under the conditions above described. The mixed ratio strongly affects the formation of the blend monolith. When the ratio of PVA/SA is 70/30, the monolith is not formed due to the very high viscosity of the solution, not suitable for the phase separation. Figure 2-2 shows the SEM images of the PVA/SA blend monolith with different mixed ratios of PVA/SA. Similar pore structures are observed in all the blend monoliths. In the case of low ratio of SA (5%), a continuous interconnected network is well formed. With increasing the content of SA, the skeleton size increases and the pore size decreases, which affects the interconnectivity of the pore structure. This behavior is explained as follows [8]. The viscosity of the solution increases with increasing the content of SA,

which leads to the higher degree of entanglement and the slower dynamics of phase separation. Furthermore, the formation of the soluble complex between PVA and SA may also delay the phase separation process.

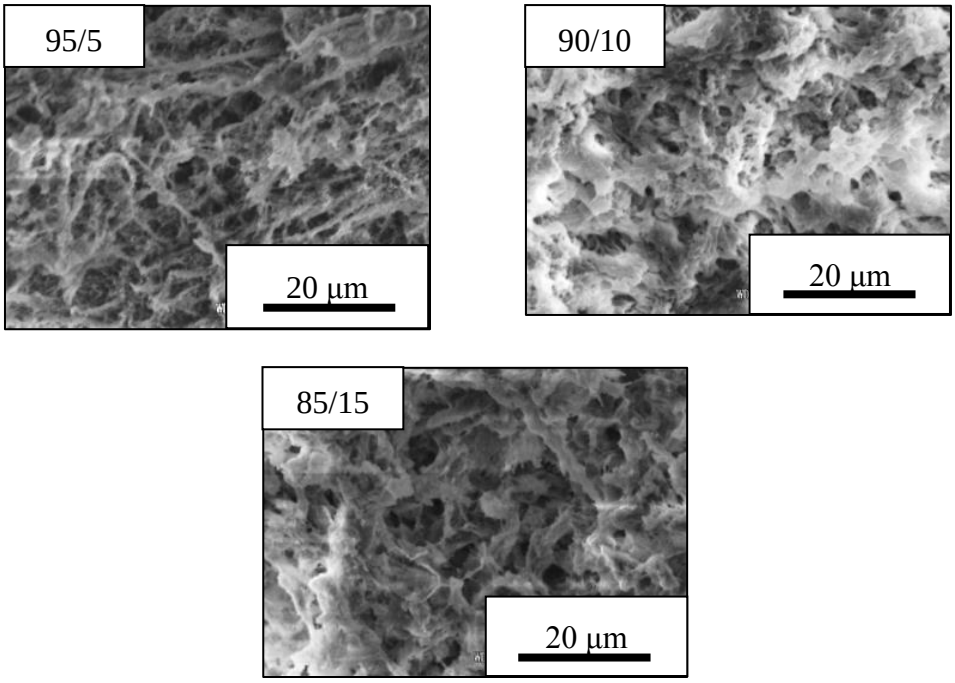


**Figure 2-2.** SEM images of PVA/SA blend monoliths with different SA contents

Nitrogen adsorption-desorption isotherm of the PVA/SA blend monolith is shown as Figure 2-3 (A). It belongs to a type II isotherm which is obtained by a macroporous absorbent. The macroporous structure can be confirmed by the SEM images which are shown as Figure 2-2. Besides, a type H3 hysteresis loop in the $P/P_0$ range from 0.5 to 1.0 is observed. This hysteresis loop is caused by capillary condensation, suggesting the existence of more or less slit-like nanoscale porous structures in the blend monolith [9]. The BET surface area of PVA/SA-1 is 89 $m^2g^{-1}$, revealing the relatively large surface area of the obtained monolith. The pore size distribution (PSD) plot of the sample

obtained by the non-local density functional theory (NLDFT) method is shown as Figure 2-3 (B). The PSD of the blend monolith is centered at 8.9 nm in the range from 5.0 nm to 26 nm. The data clearly confirms the nanoscale porous structure of the blend monolith.

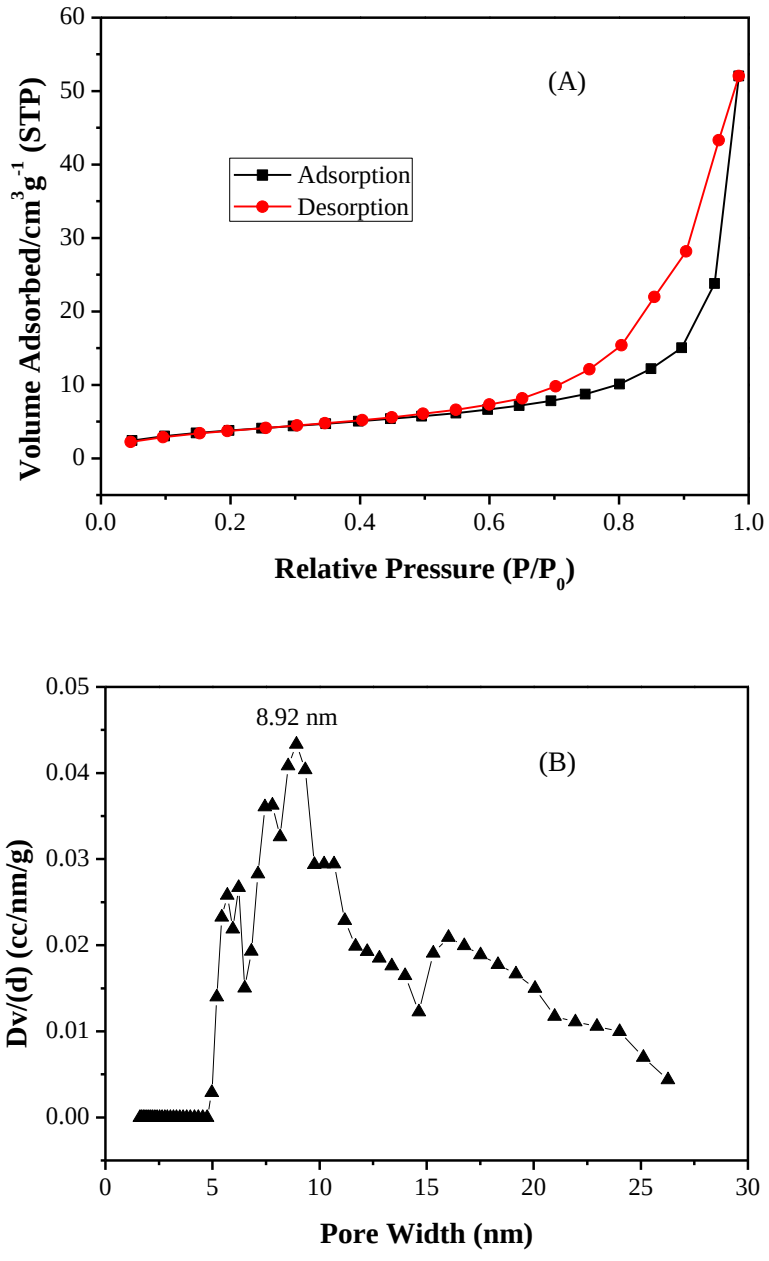


**Figure 2-3.** (A) Nitrogen adsorption-desorption isotherms of PVA/SA blend monolith (PVA/SA-1); (B) pore size distribution by NLDFT method model

The surface areas and porosity values of PVA/SA-1, PVA/SA-2, and PVA/SA-3 are shown as Table 2-1. The surface areas of PVA/SA-2 and PVA/SA-3 are 54 $cm^2/g$ and 91 $cm^2/g$ respectively, which is similar with that of PVA/SA-1. The porosity values of PVA/SA-1, PVA/SA-2, and PVA/SA-3 calculated from the equation mentioned above are 85%, 84% and 87% respectively. These data indicate that the blend monolith obtained by TINIPS method possesses relatively high surface area and very high porosity, which may be important for the potential applications.

**Table 2-1.** The surface area and porosity of blend monoliths with different mixed ratios of PVA and SA

| Code | Surface area ($cm^2g^{-1}$) | Porosity (%) |
|---|---|---|
| **PVA/SA-1** | 89 | 85 |
| **PVA/SA-2** | 54 | 84 |
| **PVA/SA-3** | 91 | 87 |

Figure 2-4 shows FT-IR spectra of PVA, SA, and the blend monolith (PVA/SA-3), which clearly implies that the blend monolith consists of both polymers. In the spectrum of SA, peaks at 1600 $cm^{-1}$ and 1410 $cm^{-1}$ are ascribed to asymmetric and symmetric carboxylate stretching vibrations of SA, respectively. These two vibrations are also observed in all the spectra of the blend monoliths and shift to a higher frequency range. These data clearly suggest the strong interaction between PVA and SA in the blend monolith [6]; the hydrogen bond between the carboxyl group of SA and hydroxyl group of PVA is formed. This interaction may be related to the specific solvent of the phase

separation for the combination of PVA and SA.

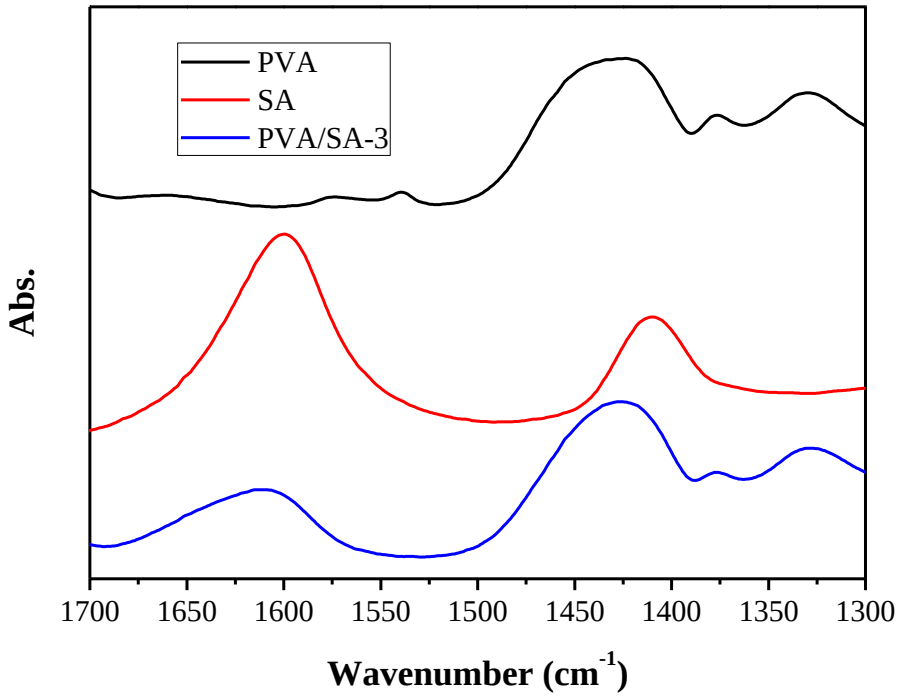


**Figure 2-4.** FT-IR spectra of PVA, SA, and the PVA/SA monolith (PVA/SA-3)

The pH-sensitive property of the PVA/SA blend monolith with different mixed ratios is shown in Figure 2-5. At first, the dried blend monolith is placed in an acidic solution (pH=1.0). The monolith is gradually swollen. After 9 h, the sample is transferred into in a neutral solution (pH 7.4). Under the acidic condition, the swelling ratio decreases with increasing the SA content; while the swelling ratio significantly increases as the SA content increases under the neutral condition. This behavior can be explained by the acidic form of the carboxylate group of SA in pH 1.0 and the neutralized form in pH 7.4; the electrostatic repulsion of the carboxylate group increases, leading to the increase of the swelling ratio [10-12].

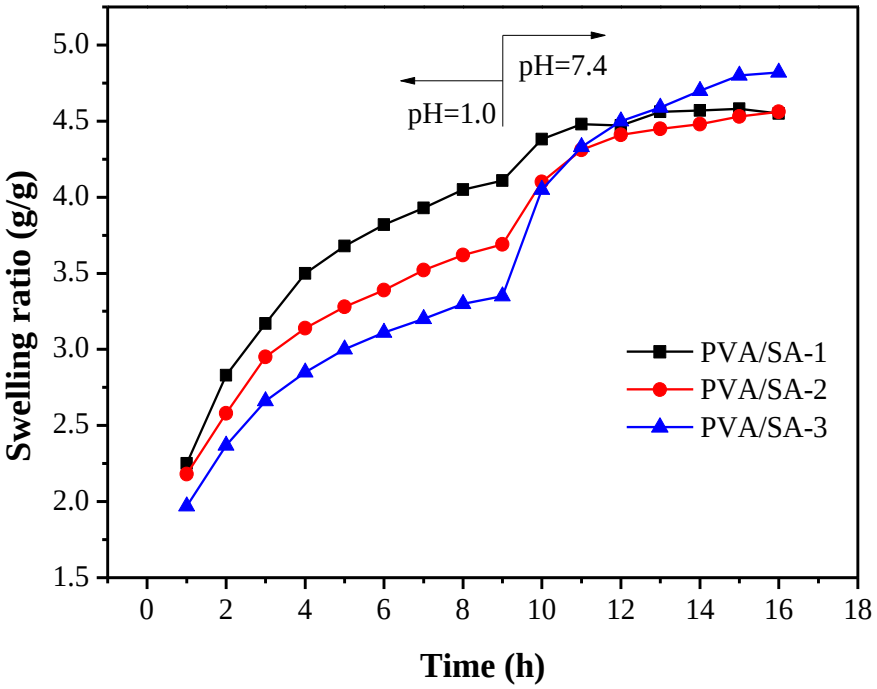


**Figure 2-5.** Effect of pH on swelling behaviors of PVA/SA blend monoliths

## 2.4 Conclusion

The PVA/SA blend monolith with nanoscale porous structure and pH-responsive property is successfully fabricated via TINIPS without any templates. We have first achieved the fabrication of a monolith containing SA by the appropriate selection of the solvent for the phase separation.

PVA and SA are widely used as biomaterials due to their good biocompatibility. A combination of this feature and nanoscale structural characteristics of the present blend monolith offers promising prospects for the applications in bio-related and environmental fields. SA provides the pH-sensitive property in the blend monolith, which may be potentially useful for controlled drug delivery systems. Moreover, the present study is highly significant to suggest the possibility to fabricate blend monoliths

consisting of bioactive polymers which cannot form monolithic structure solely. Further studies on the fabrication of blend monoliths of functional polymers and their bio-related applications are under way in our laboratory.

## 2.5 Reference


1. Wei X, Qi L, Yang G, Wang F, *Talanta* 2009, **79**, 739.
2. Hanora A, Savina I, Plieva FM, Izumrudov VA, Mattiasson B, Galaev IY, *J. Biotechnol.* 2006, **123**, 343.
3. Xin Y, Uyama H, *Chem. Lett.* 2012, **41**, 1509.
4. Safi S, Morshed M, Hosseiini Ravandi SA, Ghiaci M, *J. Appl. Poly. Sci.* 2007, **104**, 3245.
5. Coleman MM, Painter PC, *Prog. Polym. Sci.* 1995, **20**, 1.
6. Dong YQ, Zhang L, Shen JN, Song MY, Chen HL, *Desalination* 2006, **193**, 202.
7. Braccini I, Pérez S, *Biomacromolecules* 2001, **2**, 1089.
8. Gopishetty V, Tokarev I, Minko S, *J. Mater. Chem.* 2012, **22**, 19482.
9. Sing KSW, *Pure Appl. Chem* .1982, **54**, 2201.
10. Lin Y, Liang Chung HC, Chen M, Sung H, *Biomaterials* 2005, **26**, 2105.
11. Xia C, Xiao C, *J. Appl. Polym. Sci.* 2012, **123**, 2244.
12. Xie L, Jiang M, Dong X, Bai X, Tong J, Zhou J, *J. Appl. Polym. Sci.* 2012, **124**, 823.

# Chapter 3

# In Situ Mineralization of Hydroxyapatite on Poly(vinyl alcohol) Monolithic Scaffolds for Tissue Engineering

## 3.1 Introduction

In the 1970s and 1980s, tissue engineers began working on growing replacement organs for transplantation into patients. Up to now, various strategies have been developed in order to regenerate tissues such as bone, cartilage, cornea, and skin [1-5]. For tissue engineering, autologous materials are preferred; however, their collection is often painful involving a risk of infection, nerve damage, cosmetic disability, and a loss of function [6, 7]. For this obvious reason, biodegradable polymers are expected as an excellent substitute for tissue engineering [8]. General approaches of tissue engineering require highly porous biodegradable three-dimensional (3D) scaffolds with an interconnected porous structure, which provide places for adhesion of cells and signal molecules, and facilitate nutrient and waste exchange [9].

PVA, one of the most typical hydrophilic polymers, has been used in the biomedical field due to its biocompatibility, nontoxicity, proven mechanical strength, and anabolic effect on bone formation [10-12]. Apart from these advantages, the PVA monolith with large surface area and high porosity owns interconnected porous structure. Compared to other scaffolds which are often lack of the ability to adjust the nanoscale features shown in the natural extracellular matrix (ECM), the unique property resembling the topographic features of ECM endows the PVA monolith an ideal candidate for tissue engineering [13].

Hydroxyapatite (HAp) is a major inorganic compound existing in living body. HAp possesses superior bone biocompatibility and osteoconductivity properties as well as the ability to induce calcification and form a biological bond between implant and subchondral bone [14-16], although the main defects of HAp are reported to be brittle and hard to keep its shape. Thus, HAp is usually used by combination with biocompatible polymers for application of tissue engineering.

In this study, a facile method to fabricate a PVA/HAp composite monolithic scaffold is designed and prepared for the first time. The hydroxyapatite mineralization on the PVA monolith is realized by an alternative soaking method. The effect of soaking time and soaking cycles on the aggregation of the mineral phase are investigated in detail. The PVA/HAp biocomposite monolithic scaffold with interconnected porous structure will have large potential for applications of tissue engineering.

## 3.2 Experimental

### Materials

PVA powder with a hydrolysis ratio of 98 % and a molecular weight of $8.8 \times 10^4$, calcium chloride ($CaCl_2$), sodium phosphate dibasic ($Na_2HPO_4$), and Tris-HCl solution (pH 7.5) were purchased from Wako Pure Chemical Industries, Ltd (Tokyo, Japan). A PVA monolith was prepared according to Chapter 1: PVA concentration of 60 mg/mL; acetone ratio of 43 % (vol) in the mixed solvent; cooling temperature of 20 $^{o}$C. All other reagents and solvents were used as received.

### In situ mineralization of hydroxyapatite on PVA monolith

A PVA monolith with diameter of 10 mm and height of 5 mm was immersed into

10 mL of 200 mM $CaCl_2$/Tris-HCl solution (pH 7.5) (Ca solution) for a pre-determined period of time at 37 °C. Subsequently, the monolith was taken out from Ca solution, and was soaked into 10 mL of 120 mM $Na_2HPO_4$ solution (P solution) for the same pre-determined period of time at 37 °C. These processes were repeated several times.

**The amount of hydroxyapatite formation on PVA monolith**

The amount of hydroxyapatite formed on the PVA monolith after various soaking cycles was measured as the following equation:

*Amount of hydroxyapatite formed (mg/cm$^3$) = the weight of the monolith after soaking cycles (mg)-the weight of the monolith before soaking cycles (mg)/$\pi \times 0.5^2 \times 0.5$ (cm$^3$)*

**Water uptake property**

The dried PVA/HAp composite monolith with different soaking cycles was immersed into 15 mL of water at room temperature. The weight change was measured every 30 min until the weight became almost constant. This experiment was carried out three times. The swelling ratio was calculated as follows:

$$Swelling\ ratio\ (\%) = (W_e - W_b) / W_b \times 100$$

where $W_b$ and $W_e$ were the weights of the PVA/HAp composite monolith before and after the immersion in water, respectively.

**Characterizations of HAp coated PVA monolith**

The morphology of the monolith was observed by SEM (S-3000N, Hitachi Ltd., Japan) at 15 kV. Before observation, the sample was cut with a scalpel, and was coated with a thin layer of gold by an ion sputter apparatus (E-1010 Ion Sputter, Hitachi, Japan). X-ray diffraction (XRD) patterns were obtained by a Shimadzu (Japan) XRD-6100 instrument at a scanning rate of 4.0 deg/min from 10 to 60 deg (2θ). The measurement was performed with Cu-Kalpha radiation (λ=1.5418 Å) at 40 kV/30mA. SEM in combination with energy dispersive X-ray analysis (SEM-EDX) (Miniscope TM 3000, Hitachi Ltd., Japan) was adopted to investigate the chemical composition of the composite monolith surface. The chemical structure of the monolith surface was analyzed using a Nicolet iS 5 Fourier transform infrared spectrophotometer (Thermo Scientific, Japan).

## 3.3 Results and Discussion

**Results and discussion**

Figure 3-1 shows SEM images of the PVA monolith before and after swelling in water. As shown in Figure 3-1 (A), the monolith fabricated by the phase separation has interconnected macroporous structure [17]. The PVA monolith is swollen in water by soaking for several hours, not soluble in water. The swollen PVA monolith is dried by freeze drying. After the soaking process, the pore size becomes much larger than that of before soaking. These data show that the PVA monolith is stable under the conditions of the alternating soaking for mineralization of hydroxyapatite.

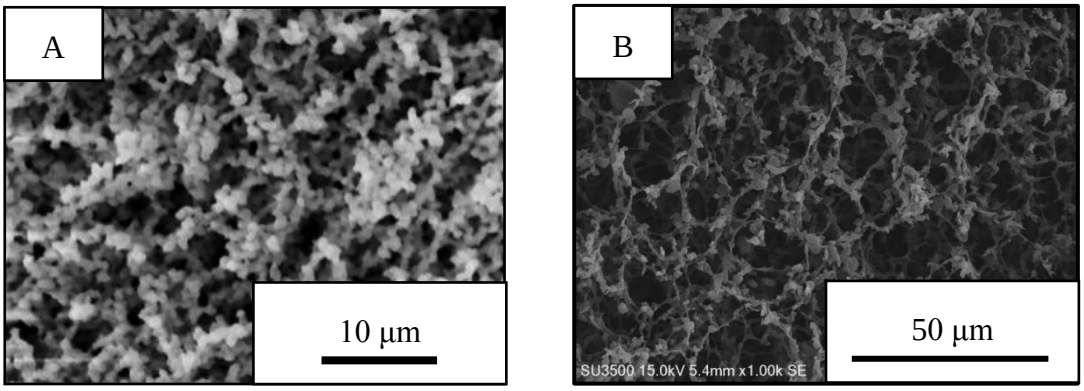


**Figure 3-1.** SEM images of PVA monolith (A) before swelling and (B) after swelling

In this study, mineralization of HAp on the monolith surface is carried out by an alternating soaking process, which is well known to be a facile method to form HAp on materials [18]. The PVA monolith is alternately soaked in a calcium ion solution and a phosphate solution with one cycle of 2 h (1 h for Ca solution, 1 h for P solution) to produce the PVA/HAp composite monolith. The morphology of the obtained monolith is observed by SEM (Figure 3-2). Flaky-like spheres attached on the monolith surface are clearly observed and the amount of such spheres increases as a function of soaking cycles. After 5 soaking cycles, the bulk formation grown on the PVA monolith is clearly observed. These data strongly suggest that HAp is mineralized on the PVA monolith.

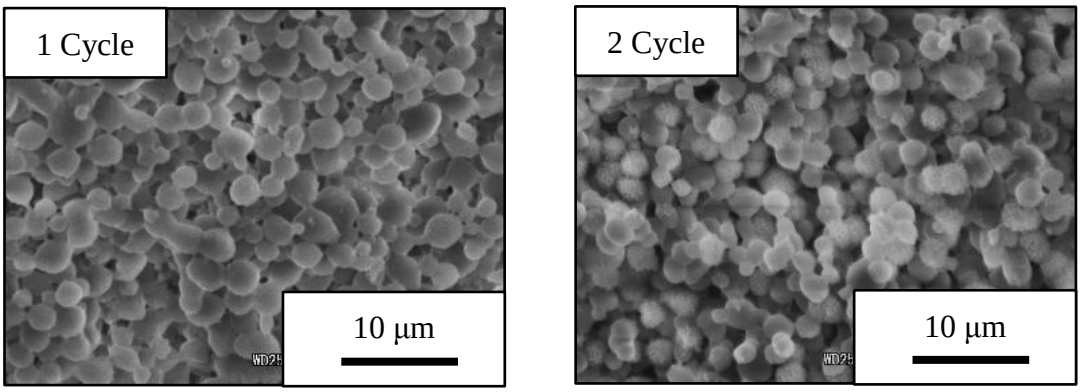

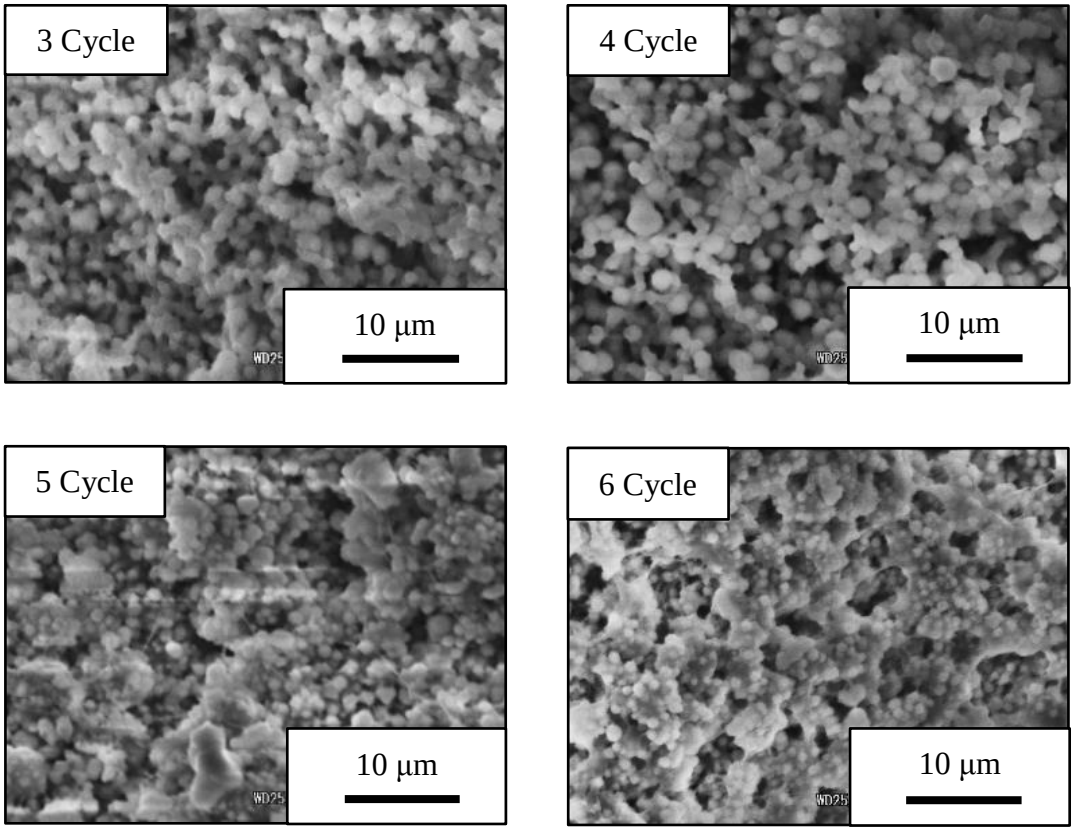


**Figure 3-2.** SEM images of PVA/HAp composite monolith with different soaking cycles

The BET surface areas of PVA/HAp composite monoliths with 2 soaking cycles and 5 soaking cycles are 68 $m^2/g$ and 27 $m^2/g$, respectively. The decrease of surface areas with the increase of soaking cycles is probably because of the bulk formation of hydroxyapatite which affects the porous structure of the composite monolith.

The obtained monolith is characterized by various analyses. The X-ray diffraction measurement is adopted to analyze the crystallinity of the product with different soaking cycles (Figure 3-3). The PVA monolith exhibits semi-crystalline structure with a large peak at a 2θ angle of 19-20 ° [19]. For the composite monolith, moreover, peaks at 26 ° and 32 ° are found, which are ascribed to the crystalline structure of HAp [8]. These peaks are more sharp and the intensity are larger as the soaking cycle increases,

suggesting that the amount of the crystalline HAp increases as a function of the soaking cycle.

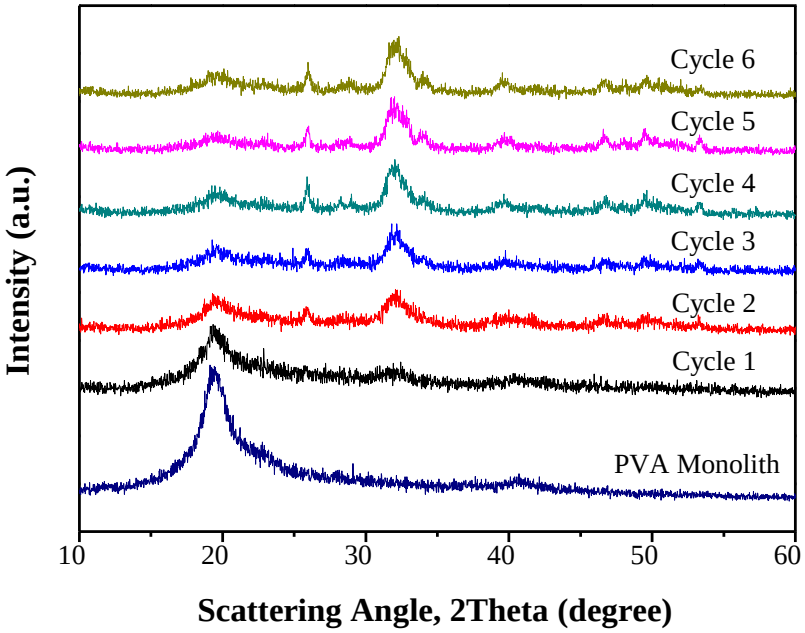


**Figure 3-3.** X-ray diffraction patterns of PVA monolith and PVA/HAp composite monolith with different soaking cycles

Figure 3-4 shows the EDX spectrum of the monolith with 6 soaking cycles in specific regions. The existence of pronounced Ca and P signals on the monolith surface is clearly observed, supporting the formation of HAp on the monolith. The Ca/P ratio determined by EDX increases as a function of the soaking cycle and reaches 1.67 after 6 cycles. This value is in good agreement with the expected stoichiometry based on the chemical structure of HAp, $Ca_{10}(PO_4)_6(OH)_2$. Besides, the detailed elemental compositions of PVA/HAp composite monoliths with 2 soaking cycles and 5 soaking cycles are shown as Table 3-1. From the table, we can observe that as the soaking cycle increases, the carbon and oxygen contents decrease and the Ca and P contents increase.

These data give evidence that as the soaking cycle increases, the formation of hydroxyapatite increases.

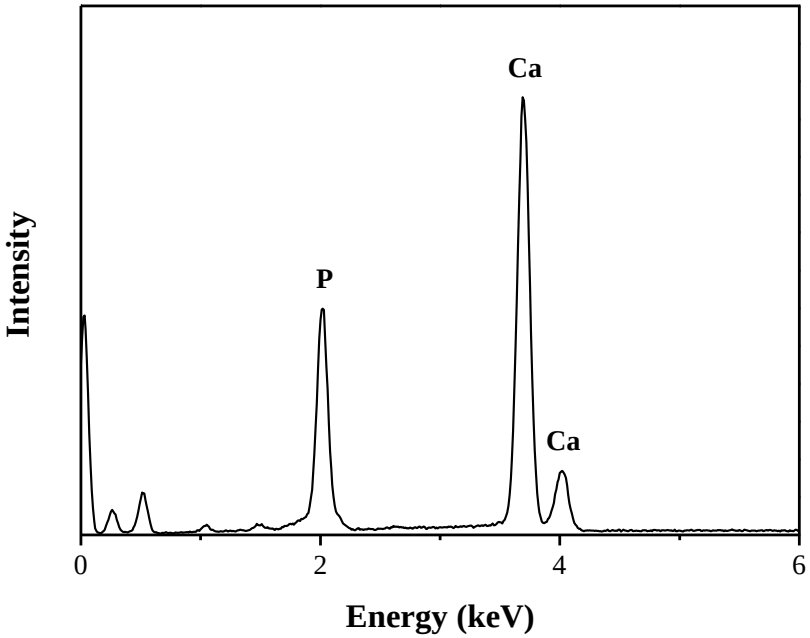


**Figure 3-4.** EDX spectrum of PVA/HAp composite monolith with 6 soaking cycle

**Table 3-1.** Detailed elemental composites of PVA/HAp composite monoliths with different soaking cycles

| **Weight content (%)** | C | O | Ca | P | Ca/P ratio |
|---|---|---|---|---|---|
| **Cycle 2** | 15.9 | 55.1 | 11.4 | 17.6 | 1.18 |
| **Cycle 5** | 12.1 | 34.0 | 17.5 | 36.4 | 1.61 |

The chemical structure of the monolith surface is examined by Fourier transform infrared spectroscopy (FT-IR). A characteristic broad peak around 3300 $cm^{-1}$ due to the

O-H stretching of PVA is found in the spectrum of the PVA monolith (Figure 3-5(A)). There are additional characteristic peaks around 1023 $cm^{-1}$ due to the P-O stretching of the phosphate group and around 560 and 600 $cm^{-1}$ ascribed to the P-O bending [9, 20]. These data strongly support the formation of HAp on the monolith surface.

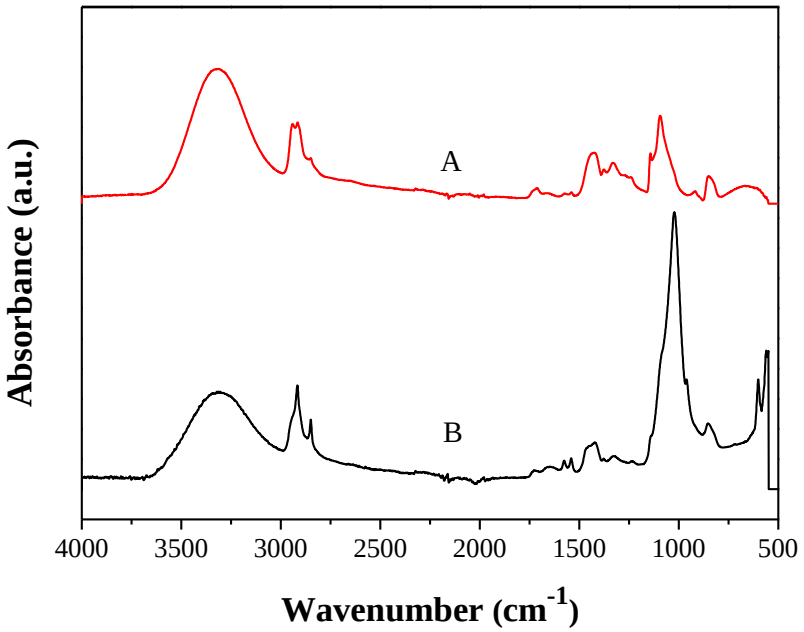


**Figure 3-5.** FT-IR spectra of (A) PVA monolith and (B) PVA/HAp composite monolith with 6 soaking cycle

Figure 3-6 presents the effects of soaking cycle and soaking time on the formation of HAp formation. The amount of HAp gradually increases as a function of soaking cycles. The relationship between the soaking cycle time and the amount of HAp is also investigated. Under the same total soaking time (8 h), the mineralization is carried out in two different kinds of soaking time, 2 h/cycle and 4 h/cycle. Shorter soaking time with more cycle number leads to larger amount of HAp. This trend is probably attributed to the diffusion of calcium ion and phosphate solution around the PVA

monolith. These results reveal that the formed amount of HAp strongly depends on the soaking cycle and soaking time.

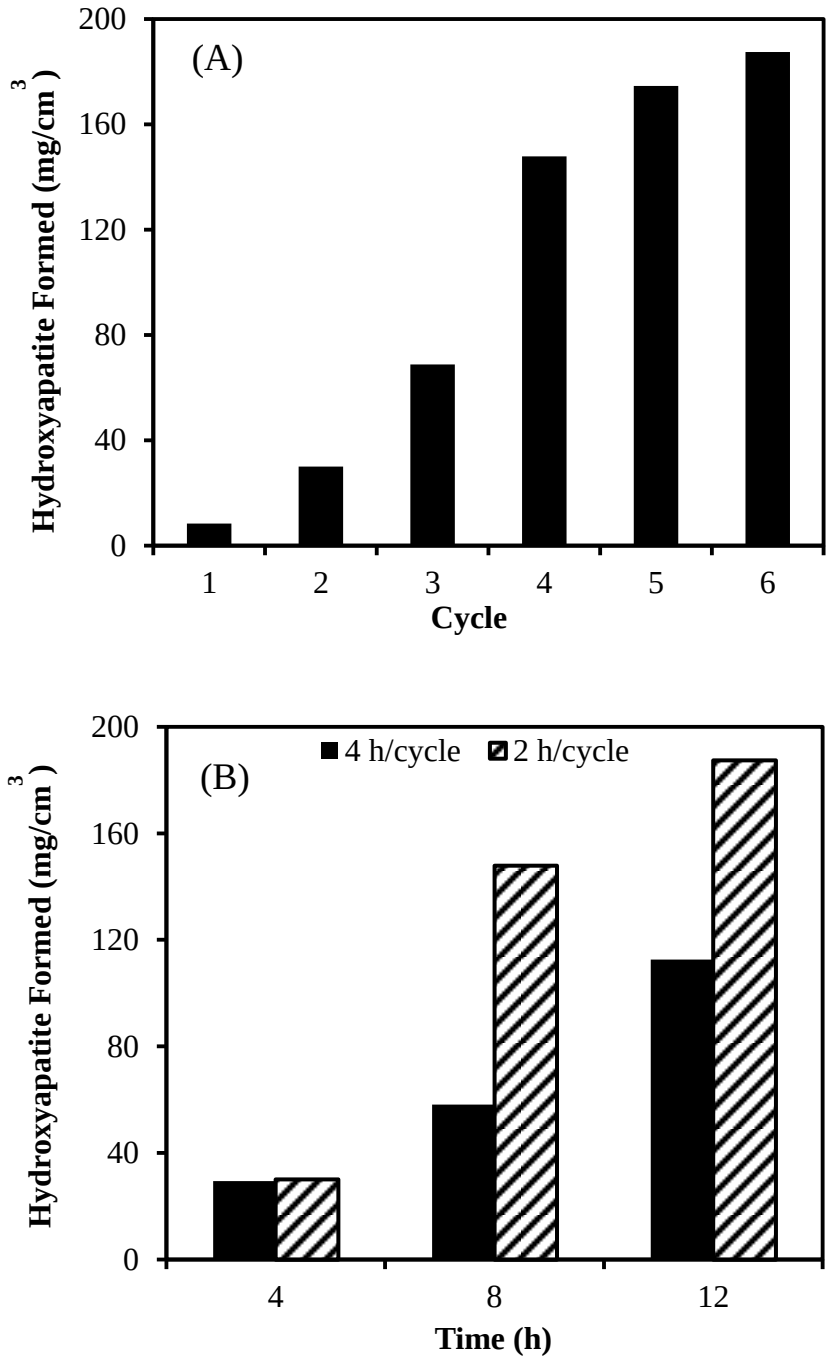


**Figure 3-6.** Effects of soaking time and soaking cycle on the amount of HAp formed on PVA monolith: (A) soaking cycle; (B) soaking time

Figure 3-7 shows the water uptake of the PVA/HAp composite monolith with different soaking cycles. Except for the case of one soaking cycle (cycle 1), the water uptake reaches to the equilibrium in a very short time (less than 3 h) and it decreases as a function of the soaking cycles. This may be explained that after one soaking cycle, the amount of HAp mineralized on the PVA monolith is too small to affect the water uptake; while for other cases, the increase of soaking cycles leads to more amount of HAp on the monolith, resulting in the lower water uptake. These data clearly shows that the hydrophilic property of the monolith can be easily controlled by the mineralization of HAp on the PVA monolith, which is important for the scaffold application of tissue engineering.

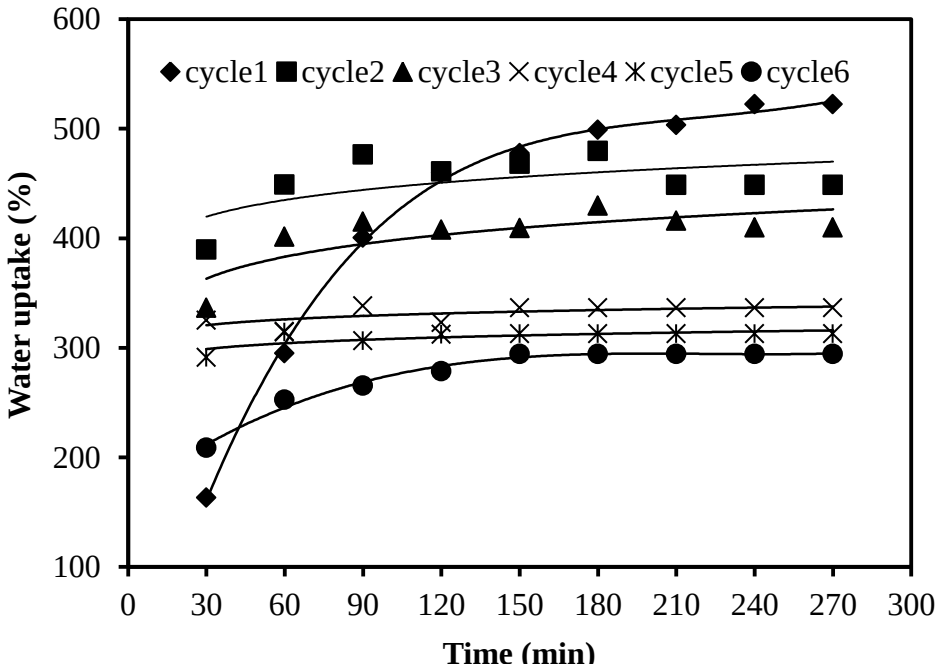


**Figure 3-7.** Water uptake of PVA/HAp composite monolith with different soaking cycles

## 3.4 Conclusion

A novel PVA/HAp composite monolithic scaffold is successfully fabricated via thermally impacted non-solvent induced phase separation method in the combination of an alternate soaking process for the first time. The morphology observation of the PVA/HAp composite monolith shows that HAp is successfully mineralized onto the surface of the PVA monolith, which is also confirmed by XRD, EDX, and FT-IR analyses. Soaking cycle and soaking time play important role in the formation of HAp. With the increase of soaking cycle and soaking time, the amount of HAp formed increases. The water uptake of the composite monolith decreases as a function of the soaking cycle, strongly suggesting the less hydrophilic nature of the monolith by the mineralization of HAp.

The present PVA-based composite monolith has potential merits based on the properties of PVA and monolithic structure as well as features of HAp such as good affinity for cells and biomolecules, biocompatibility, and osteoconductivity. Therefore, scaffold of bone tissue engineering is a strong candidate for applications of the present composite monolith. Further studies on the application of the PVA/HAp composite monolith for scaffold are under way in our laboratory.

## 3.5 Reference


1. Krenkova J, Frerich B, Lenz S, Tiede S, Buchmeiser MR, *Macromol. Rapid Commun.* 2010, **31**, 1540.
2. Laurencin CT, Attawia MA, Elgendy HE, Herbert KM, *Bone* 1996, **19**, 93S.
3. Temenoff JS, Mikos AG, *Biomaterials* 2000, **21**, 431.
4. Rafat M, Li F, Fagerholm P, Lagali NS, Watsky MA, Munger R, Matsuura T,

Griffith M, *Biomaterials* 2008, **29**, 3960.

5. Ma L, Gao C, Mao Z, Zhou J, Shen J, Hu X, Han C, *Biomaterials* 2003, **24**, 4833.
6. Petite H, Viateau V, Bensaïd W, Meunier A, Pollak C de, Bourguignon M, Oudina K, Sedel L, Guillemin G, *Nature Biotechnol.* 2000, **18**, 959.
7. Damien CJ, Parsons JR, *J. Appl. Biomater.* 1991, **2**, 187.
8. Martina M, Hutmacher DW, *Polym. Int.* 2007, **56**, 145.
9. Thomas V, Dean DR, Jose MV, Mathew B, S, *Biomacromolecules* 2007, **8**, 631.
10. Sailaja GS, Sreenivasan K, Yokogawa Y, Kumary TV, Varma HK, *Acta Biomater*.2009, **5**, 1647.
11. Cha W, Hyon S, Oka M, Ikada Y, *Macromol. Symp.* 1996, **109**, 115.
12. Song W, Markel D, Wang S, Shi T, Mao G, Ren W, *Nanotechnology* 2012, **23**, 115101.
13. Li D, Xia Y, *Adv. Mater.* 2004, **16**, 1151.
14. Watanabe J, Akashi M, *Biomacromolecules* 2006, **7**, 3008.
15. Lee W, Zavgorodniy AV, Loo C, Rohanizadeh R, *J. Biomed. Mater. Res. Part A* 2012, **100A**, 1539.
16. Wang M, Li Y, Wu J, Xu F, Zuo Y, Jansen JA, *J. Biomed. Mater. Res. Part A* 2008, **85A**, 418.
17. Sun X, Fujimoto T, Uyama H, *Polym. J* .2013, **45**, 1101.
18. Taguchi T, Kishida A, Akashi M, *Chem. Lett* .1998, 711.
19. Bunn CC, *Nature* 1948, **161**, 929.
20. Wu G, Su B, Zhang W, Wang C, *Mater. Chem. Phys*. 2008, **107**, 364.

# Chapter 4

# Fabrication of Acetoacetylated Poly(vinyl alcohol) Monolith via Thermally Impacted Non-Solvent Induced Phase Separation for Enzyme Immobilization

## 4.1Introduction

Enzyme immobilization was first described almost 100 years ago and its systematic investigation began from the mid-1960s [1, 2]. It is one of the leading techniques employed in biotechnology and bioengineering due to its low cost-to-benefit ratios of real-world processes based on such biocatalytic systems. Besides, enzyme immobilization on a solid support owns other advantages. For example, it enhances the stability of enzyme and enables it for continuous use; the reaction can be stopped immediately after the reaction mixture leaves the reactor, as well as the product can be easily removed from the reaction mixture and cannot be contaminated with the biocatalyst [3-5].

Up to now, there is a variety of immobilization approaches which have been reported. Typical immobilization techniques can be divided into two groups: physical methods including adsorption and entrapment in a polymeric structure (gel, membrane, capsule, fiber,); and chemical reactions such as ion exchange and covalent attachment. Among these methods, the covalent binding of enzyme to a support has received increasing attention because it can form strong and stable linkages between the enzyme and the support, and it can also eliminate the loss of activity by enzyme leakage from the support [6-13].

Generally, the ideal supports for the immobilization of free enzymes should possess specific properties, such as large surface area for the immobilization of huge amount of enzymes, rapid mass transport, as well as excellent chemical and mechanical stability [14, 15].

Porous polymer monoliths developed in the early 1990s are the newest contribution to the family of enzyme immobilization supports due to their excellent properties, such as high permeability, large through-pores, rapid mass transport, stability in most solvents, and versatility of functional group available on the pore surface of the monoliths.

In this study, an acetoacetylated PVA monolith is synthesized by TINIPS method and modified for the enzyme immobilization. Acetoacetylated PVA with acetoacetyl groups is usually used as adhesive (Figure 4-1) [16, 17]. Here, we just make use of the acetoacetyl groups which are suitable for modification to realize the enzyme immobilization.

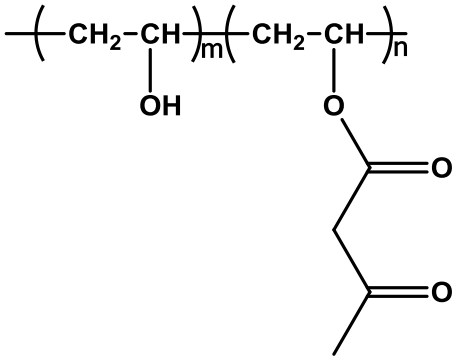


**Figure 4-1.** Chemical Structure of AAPVA

## 4.2 Experimental

### Materials

Acetoacetylated PVA powders with hydrolysis ratio of 99 % and the molecular weight of 44,000 were used as received. Polyetherimide with the molecular weight of 10,000, glutaraldehyde (GA) solution (25 wt%) , lipase and horseradish peroxidase (HRP) were purchased from Wako Pure Chemical Industries, Ltd. Other reagents and solvents were used as received.

### Measurements

The microstructure of PVA monolith was observed by scanning electron microscopy (SEM) (S-3000N SEM, Hitachi, Japan) at 15 kV. Before observation, the sample was cut with a scalpel, and was coated with a thin layer of gold by an ion sputter apparatus (E-1010 Ion Sputter, Hitachi, Japan). The Brunauer Emmett Teller (BET) method was utilized to determine specific surface areas. Before the measurements, all samples were degassed at 25 $^{o}$C for 12 h under vacuum. Fourier transform infrared spectroscopic (FT-IR) spectra were recorded by Nicolet iS 5 (Thermo Scientific, Japan).

### Preparation of AAPVA monolith

AAPVA powder was firstly dissolved into distilled water at 95 ºC for about 4 h with constant stirring at 400 rpm to form a homogeneous aqueous AAPVA solution. The solution was then cooled to 55 ºC, and acetone (non-solvent) was added dropwise to avoid the formation of precipitates. Afterward the mixture was kept at 20 ºC for 24h, at which period the phase separation took place to form a white monolithic material. The solvent in the monolith was replaced with acetone by immersion of the monolith into 60

mL of acetone for 12 h under gentle shaking. The solvent replacement was repeated three times and the monolith was finally dried in vacuo.

**Modification of AAPVA monolith**

AAPVA monolith was aminated by treating it with excess of polyethylenimine (PEI) ethanol solution. The AAPVA monolith was submerged in 10mL of PEI ethanol solution (40 mg/mL ) for 24 h at room temperature. The monolith was then rinsed with ethanol for 3 times to remove the excess PEI. The aminated AAPVA monolith was dried in vacuo for 24 h. PEI modified AAPVA monolith was then activated using 20 mL of glutaraldehyde (GA). The PEI modified monolith was immersed into aqueous solution of GA (1 wt%) at 40 °C for 1 h under stirring at pH 8. After completion of the activation process, the obtained monolith was taken out and washed by distilled water to remove unreached glutaraldehyde. And then the obtained monolith was dried by freeze drying.

**Immobilization of Lipase and Horseradish Peroxidase on AAPVA monolith**

Lipase and horseradish peroxidase (HRP) solutions were prepared by adding appropriate amount of lipase and HRP powder to 50 mM of phosphate buffer solution (pH 7), respectively. A designed weight of monolith was submerged in 1 mL of enzyme solution at 4 °C for 24 h.

**Activity of lipase and HRP immobilized modified AAPVA monolith**

Lipase activity was determined as follows. The reaction media was prepared by mixing 1 mL of ethanol containing 5 mg p-NPP and 1 mL phosphate buffer (50mM, pH 7.5). The lipase immobilized monolith was added into the mixture at 35 °C for 5 min.

Afterwards 2 mL $Na_2CO_3$ solution (0.5 M) was added to terminate the reaction. The color changes of the solution were checked [18, 19].

For HRP immobilization activity, the HRP immobilized modified AAPVA monolith was immersed in 25 mL colorless solution consisting of a mixture of 5 mL phosphate buffer (50mM, pH 7.0), 10 mL phenol (PhOH, 172 mM)-4-aminoantipyrine (4-AAP, 2.46 mM) mixture and 10 mL $H_2O_2$ (2mM). The color changes of the solution were observed [20].

## 4.3 Results and Discussion

### Fabrication of AAPVA monolith

The general synthetic procedure is shown as Figure 4-2. For the fabrication process, selection of non-solvent and the ratio of solvent and non-solvent are crucial factors for the formation of the blend monolith. The detailed screening of the phase separation solvent shows that a mixture of water and acetone with ratio of 10:9 is the most suitable. When the water and acetone ratio is lower than 10:9, the precipitation takes place very quickly, resulting in no formation of the monolith. On the other hand, no phase separation occurs when the ratio is more than 10:9. These behaviors can be rationalized as follows. After adding ethanol into the polymer solution, the mixed solvent system transforms into polymer-rich phase and polymer-lean phase. As the amount of non-solvent (acetone) increases, the polymer segments in the polymer-rich phase become folded and aggregated, leading to the increase of the concentration in the polymer-rich phase. When the increasing concentration reaches to a certain degree, the phase separation takes place. In the case of smaller amount of non-solvent, the concentration of polymer-rich phase is not high enough to induce the phase separation;

while for much larger amount of non-solvent, a mass of polymer segments aggregate rapidly, resulting in precipitation of the polymer in the phase separation system.

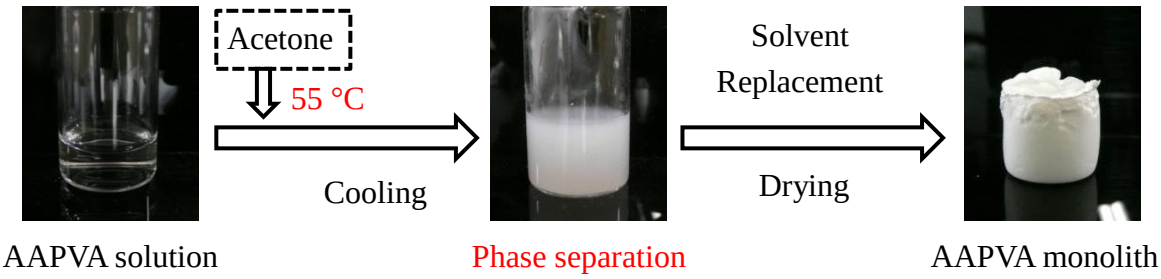


**Figure 4-2.** Fabrication process of AAPVA monolith via TINIPS method

The morphology of the AAPVA monoliths with different AAPVA concentrations is shown as Figure 4-3. In all the cases examined, relatively uniform skeleton is formed. In this system, polymer concentration is vital important for the formation of AAPVA monolith. When the polymer concentration is below 100 mg/mL, no monolith forms, as well as that of upper than 180 mg/mL. It is probably due to the viscosity of the system. When the polymer concentration is too low, the viscosity of the system is too low to induce the phase separation to form the monolith; while when the polymer concentration is too high, the high viscosity affects the diffusion of the non-solvent in the solution, resulting in the failure of phase separation as well.

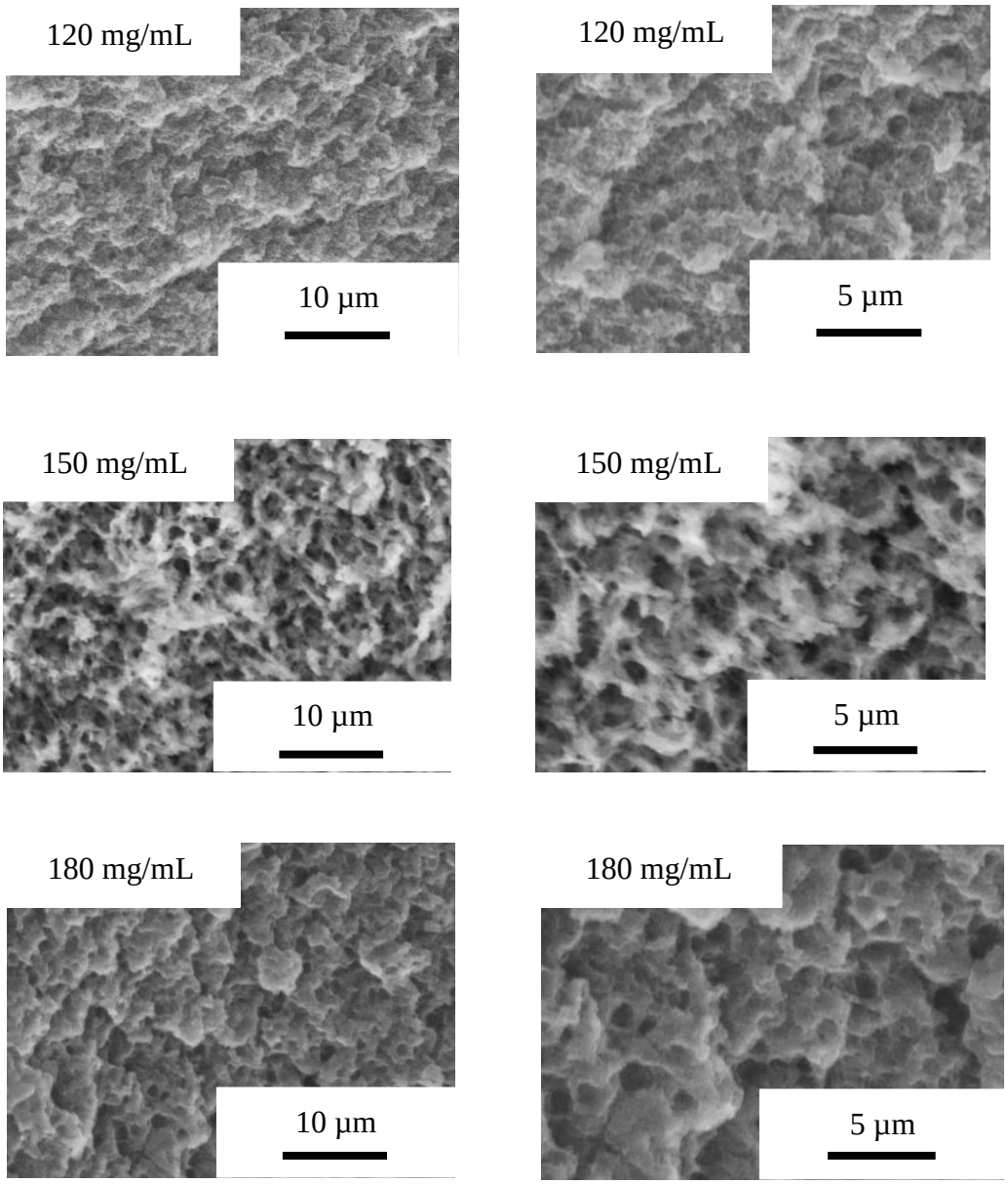


**Figure 4-3.** SEM images of AAPVA monolith with different polymer concentrations

Moreover, the morphology of AAPVA monolith is also affected by the cooling temperature. Figure 4-4 shows the morphology of AAPVA monoliths under different cooling temperatures. When the cooling temperature is -20 °C, the pore size is much smaller than that of under the cooling temperature of 20 °C. This could be explained as

follows. At high temperature, the polymer chains can move more freely and have long enough time to coagulate to form the monolith with larger pore size, whereas at lower temperature, the movement of the polymer chains is limited and the phase separation takes place very quickly, leading to smaller pore size.

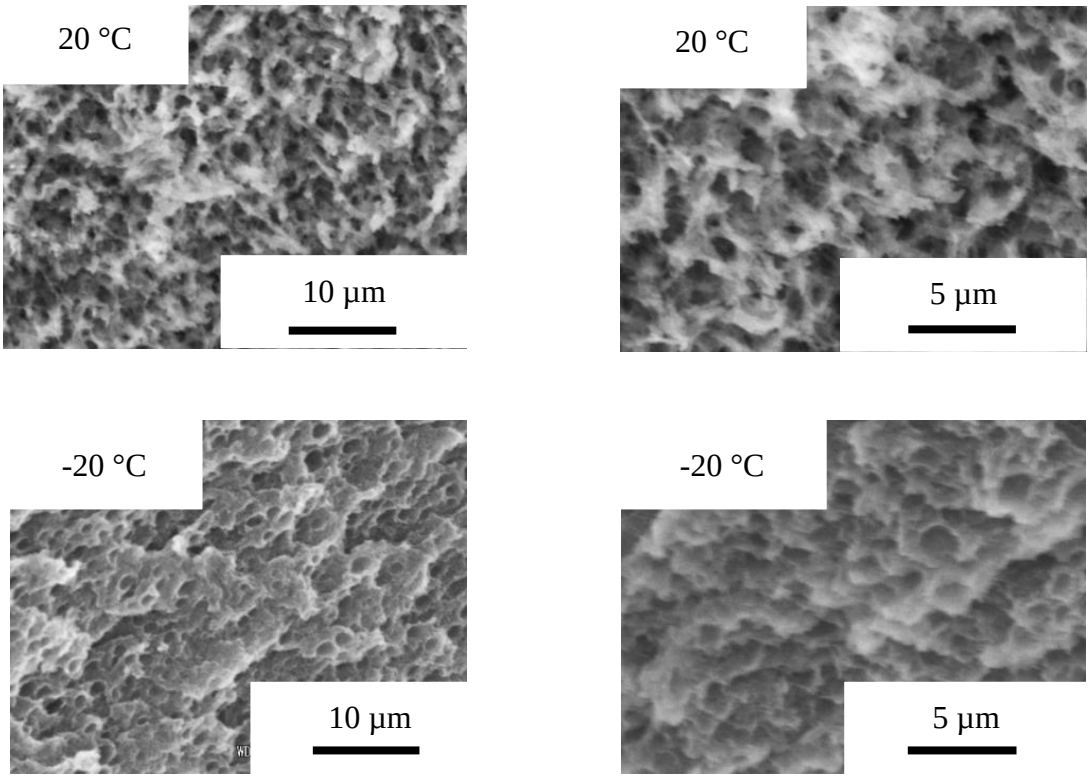


**Figure 4-4.** SEM images of AAPVA monolith with different cooling temperatures

The adsorption-desorption isotherm of the AAPVA monolith is shown in Figure 4-5. The isotherm is ascribed to type IV demonstrating mesopores exist in the monolith. The isotherm at the beginning is of monolayer adsorption, followed by multilayer adsorption, and the hysteresis in the multilayer range is associated with capillary

condensation in mesopore structures. The hysteresis loop in the $P/P_0$ range from 0.7 to 1.0 is of type H1 that means the AAPVA monolith contains cylindrical pores with narrow distributions of pore size. The BET surface area of AAPVA monolith is 81 $m^2/g$, revealing relatively large surface area.

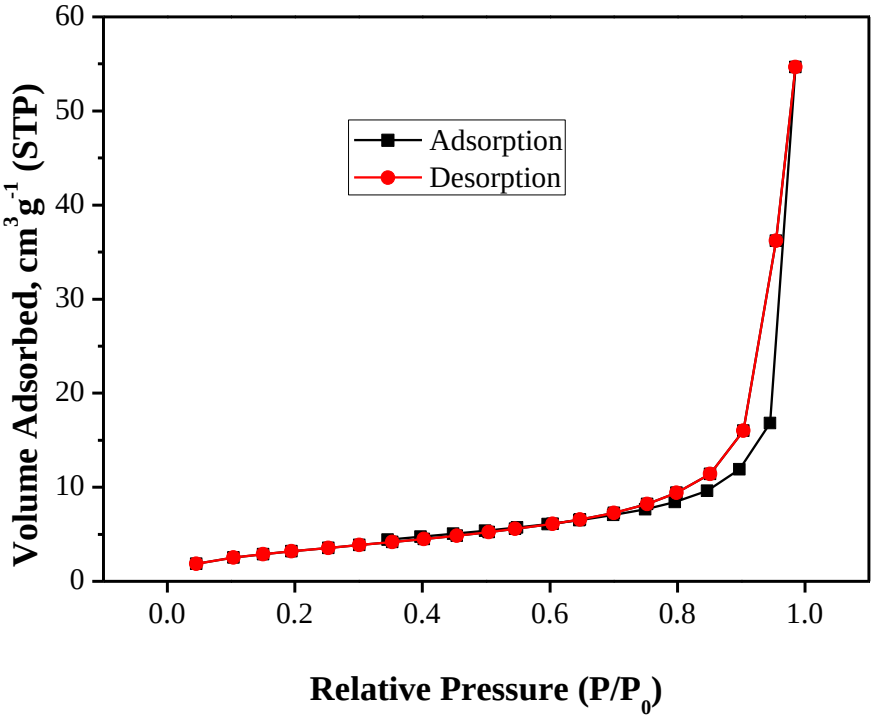


**Figure 4-5.** Nitrogen adsorption/desorption isotherms of AAPVA monolith

**Modification of AAPVA monolith**

In this study, AAPVA monolith with acetoacetyl groups is selected to be modified with PEI and GA to be used as support for lipase and HRP immobilization. The modification process includes two steps, which is shown as Scheme 4-1. At first, the monolith is modified with PEI in order to introduce amine groups to its structure. PEI is a water-soluble polycation consisting of primary, secondary and tertiary amine groups.

After this reaction, the aminated surface of AAPVA monolith is formed. Afterwards, GA, a popular reagent for enzyme immobilization, is adopted to react with amine groups to introduce aldehyde group onto the monolith. The introduced aldehyde group can be used for the enzyme immobilization. Figure 4-6 shows the SEM images of AAPVA monolith before (A) and after (B) modification. It can be found that the porous structure of the monolith maintains after the modification.

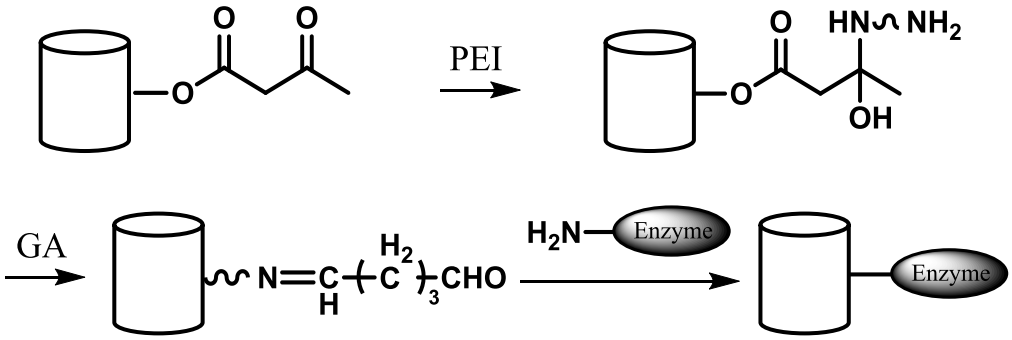


**Scheme 4-1.** Synthesis of modified AAPVA monolith with PEI and GA for enzyme immobilization

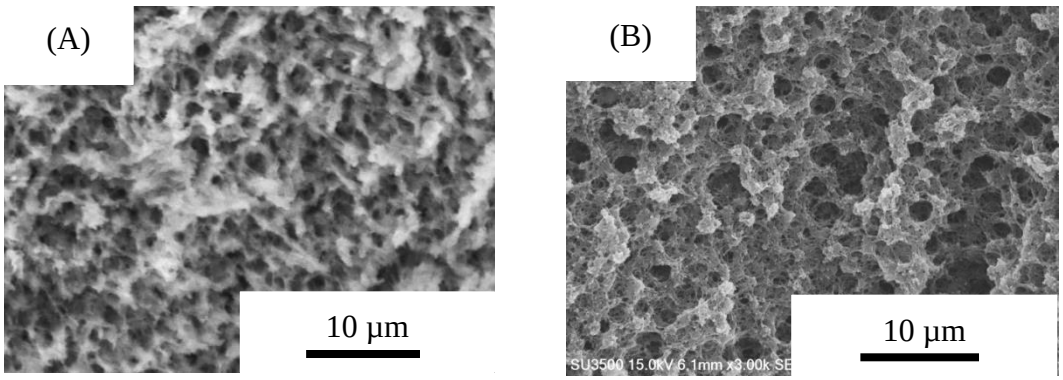


**Figure 4-6.** SEM images of AAPVA monolith before (A) and after (B) modification

Figure 4-7 shows the FT-IR spectra of AAPVA monolith before and after modification with PEI (PEI-modified AAPVA monolith) and GA (GA/PEI-modified

AAPVA monolith). As shown in Figure 4-7 (A), the structure of the AAPVA monolith is characterized by typical absorption bands at around 1680 $cm^{-1}$ for C=O. In Fig. 4-7 (B), the new appeared absorption band at the peak around 1640 $cm^{-1}$ represents the existence of amine groups after modification of PEI. According to Figure 4-7 (C), a new peak appeared around at 1700 $cm^{-1}$ responds to the existence of CHO groups after the reaction between PEI and GA. The FT-IR results show that the aldehyde groups are successfully grafted onto the AAPVA monolith.

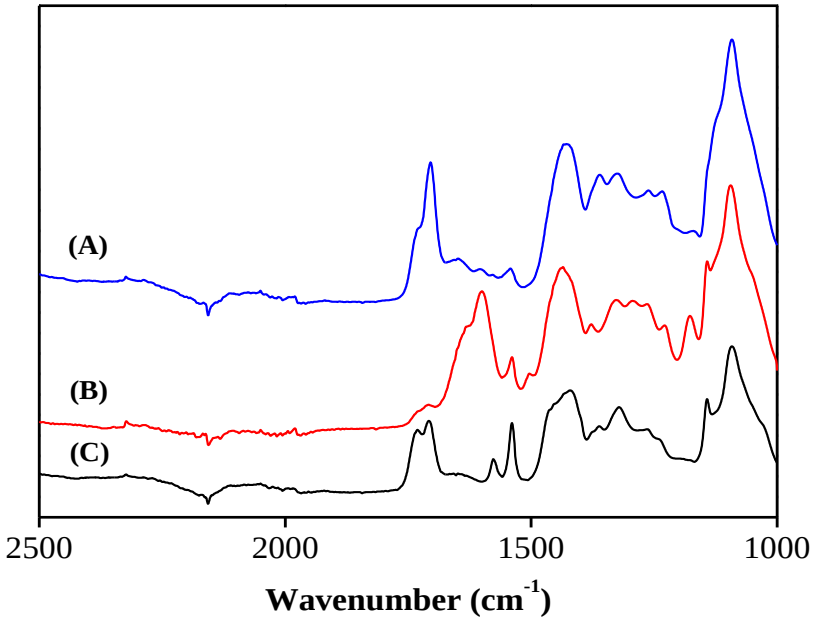


**Figure 4-7.** FT-IR spectra of AAPVA monolith (A), PEI-modified AAPVA monolith (B) and GA/PEI-modified AAPVA monolith (C)

**Enzyme immobilization**

In this study, lipase and horseradish peroxidase (HRP) are adopted to investigate the enzyme immobilization property of the modified AAPVA monolith. The

immobilized amounts of enzyme are shown as Figure 4-8. It is clearly shows that there is relatively high immobilized amount of both lipase and HRP. The amounts of immobilized lipase and HRP are 28.6 mg/g and 31.4 mg/g, suggesting the modified AAPVA monolith owns excellent immobilization property. For the lipase activity, after the reaction, the color of the solution is changed from colorless to yellow which identifies the activity of the immobilized lipase. And for the HRP activity, the color of the solution changes from colorless to red revealing the immobilized HRP also owns activity.

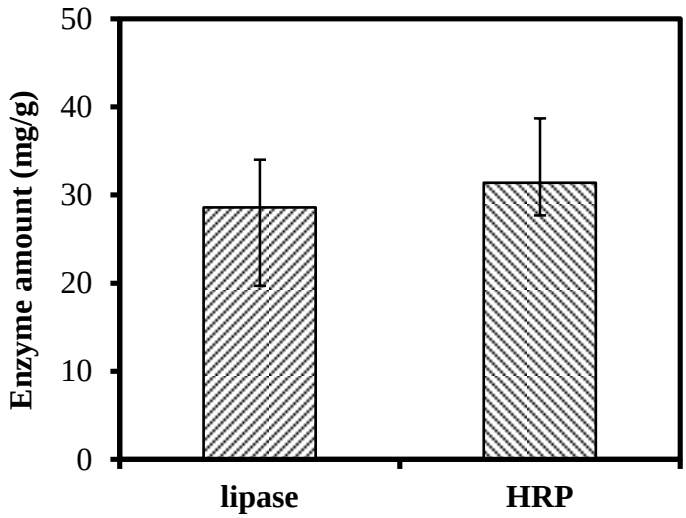


**Figure 4-8.** Immobilization amount of enzyme onto the modified AAPVA monolith

## 4.4 Conclusion

An AAPVA monolith is fabricated through TINIPS method successfully. The results of SEM suggest that AAPVA monolith owns relatively uniform pore structure. By changing the polymer concentration and the cooling temperature, the porous structure can be easily tuned. The AAPVA monolith is modified with PEI, subsequently with GA. After the modification, aldehyde groups are grafted onto the AAPVA monolith

successfully. The obtained monolith is used as enzyme immobilization support. Lipase and HRP are immobilized on the modified monolith successfully, and the activities of the enzymes are also investigated. The resultant modified monolith has large potential for enzyme immobilization.

## 4.5 Reference


1. Alwael H, Connolly D, Clarke P, Thompson R, Twamley B, O'Connor B, Paull B, *Analyst* 2011, **136**, 2619.
2. Al-Zuhair S, *Biofuels Bioprod. Bioref* .2007, **1**, 57.
3. Giorno L, Drioli E, *Trends Biotechnol.* 2000, **18**, 339.
4. Rios GM, Belleville MP, Paolucci D, Sanchez J, *J. Membr. Sci.* 2004, **242**, 189.
5. Paolucci-Jeanjean D., Belleville MP, Rios GM, Zakhia N, *Biochem. Eng. J.* 2000, **5**, 17.
6. Wang Y, Hsieh YL, *J. Membr. Sci.* 2008, **309**, 73.
7. Donato L, Algieri C, Miriello V, Mazzei R, Clarizia G, Giorno L, *J. Membr. Sci.* 2012, **407-408**, 86.
8. Sen D, Sarkar A, Gosling A, Gras SL, Stevens, Kentish SE, Bhattacharya PK, Barber AR, Bhattacharjee C, *J. Membr. Sci.* 2011, **378**, 471.
9. Mei L, Xie R, Yang C, Ju XJ, Wang JY, Zhang Z, Chu LY, *J. Membr. Sci.* 2013, **429**, 313.
10. Ren G, Yu H, *Biochem. Eng. J.* 2011, **53**, 286.
11. David AE, Wang NS, Yang VC, Yang AJ, *J. Biotechnol.* 2006, **125**, 395.
12. Ghosh S, Chaganti SR, Prakasham RS, *J. Mol. Catal. B Enzym.* 2012, **74**,132.

13. Mei L, Xie R, Yang C, Ju XJ, Wang W, Wang JY, Chu LY, *Chem. Eng. J.* 2013, **232**, 573.
14. Parthasarathy RV, Martin CR, *Nature* 1994, **369**, 298.
15. Tischer W, Wedekind F, *Top Curr. Chem.* 1999, **200**, 95.
16. Mori A, Kitayama T, Takatani M, Okamoto T, *J. Appl. Polym. Sci.* 2004, **91**, 2966.
17. Hori N, Asai K, Takemura A, *J. Wood Sci.* 2008, **54**, 294.
18. Ye P, Kang XZ, Wu J, Innocent C, Seta P, *Biomaterials* 2006, **39**,1041.
19. Yi SS, Noh JM, Lee YS, *J. Mol. Catal. B: Enzym.* 2009, **57**, 123.
20. Wang D, Sun G, Xiang B, Chiou BS, *Eur. Polym. J.* 2008, **44**, 2032.

## Concluding Remarks

This thesis deals with the fabrication of poly(vinyl alcohol)-based monoliths by TINIPS method. Through appropriate modification, these materials can be utilized in various fields. The results obtained through this study are summarized as follows.

In Chapter 1, the first successful fabrication of PVA monolith with interconnected porous structure via TINIPS method is demonstrated. The resultant PVA monoliths possess relatively large surface area and mesoporous structure. The morphology of the obtained monoliths can be easily controlled by varying the fabrication parameters. It can be observed that with the increase of molecular weight and polymer concentration, and with the decrease of cooling temperature, both the pore and skeleton sizes of the PVA monolith become smaller. In addition, the PVA monolith is successfully crosslinked with glutaraldehyde and becomes water insoluble. The swelling ratio of the monolith is decreased with the increase of GA concentration and crosslinking time.

In Chapter 2, a blend monolith consisting of PVA and sodium alginate with different mixed ratio is fabricated through TINIPS method. The SEM images show that the blend monoliths with different mixed ratios have similar porous structure, and as the increase of SA content, the skeleton size becomes larger and the pore size becomes smaller. The BET results reveal all the blend monoliths own relatively large surface area and nanoscale porous structure. The FT-IR spectra shows that there is strong interaction between PVA and SA in the blend monolith. Besides, the pH-sensitive property of the blend monolith is also certified. The TINIPS method provides a new approach to fabricated blend monoliths by selection of appropriate solvent and non-solvent.

In Chapter 3, a PVA/hydroxyapatite composite monolith is designed and prepared. The mineralization of hydroxyapatite is carried out by an alternative soaking method.

SEM images show the morphology of hydroxyapatite coated onto the PVA monolith. The results of XRD , EDX and FT-IR analysis confirm the successful mineralization of hydroxypapatite onto the PVA monolith. The soaking time and reaction cycle affect the formation amount of hydroxyapatite. As the increase of soaking time and reaction cycle, the formation amount of hydroxyapatite increases. The water uptake property of the composite monolith is significantly dependent on the amount of hydroxyapatite. As the increase of reaction cycle, the swelling ratio is decreased.

In Chapter 4, an acetoacetylated PVA monolith with acetoacetyl groups is fabricated by TINIPS. The monoliths with different AAPVA concentrations are prepared successfully. SEM images show the interconnected porous structure of the monolith. After reacting acetoacetyl groups with PEI, successively with GA, the modified AAPVA monolith is obtained. The obtained monolith shows a relatively high ability for immobilizing enzymes.

In conclusion, a series of polymer-based monoliths are prepared successfully by using PVA as the precursor and TINIPS as the fabrication techiques. The fabricated monoliths have unique three-dimensional interconnected porous structure and relatively large surface area and they are expected to find useful applications in various fields such as cell culture scaffold, tissue engineering, separation matrix as well as enzyme immobilization supports.

## List of Publications

1. Fabrication of a Poly(vinyl alcohol) Monolith via Thermally Impacted Non-solvent-induced Phase Separation
   **Xiaoxia Sun**, Takashi Fujimoto, Hiroshi Uyama
   *Polym. J.*, **2013**, 45, 1101-1106.

2. A Poly(vinyl alcohol)/Sodium Alginate Blend Monolith with Nanoscale Porous Structure
   **Xiaoxia Sun**, Hiroshi Uyama
   *Nanoscale Research Lett.*, **2013**, 8, 411-415

3. In Situ Mineralization of Hydroxyapatite on Poly(vinyl alcohol) Monolithic Scaffolds for Tissue Engineering
   **Xiaoxia Sun**, Hiroshi Uyama
   *Colloid and Polymer Science*, accepted.

4. Fabrication of an Acetoacetylated Poly(vinyl alcohol) Monolith via Thermally Impacted Non-solvent Induced Phase Separation for Enzyme Immobilization
   **Xiaoxia Sun**, Hiroshi Uyama
   In preparation.

## Acknowledgements

Completing my Ph.D. degree is probably the most challenging activity of my first 27 years of my life. The best and worst moments of my doctoral journey have been shared with many people. It has been a great privilege to spend 3 years in the Department of Applied Chemistry at Osaka University, and its members will always remain dear to me.

First and foremost I would like to express my sincerest gratitude to my supervisor Prof. Uyama for the continuous support of my PhD study and research. He patiently provided the vision, encouragement and advice necessary for me to proceed through the doctoral program and complete my dissertation. He has always made himself available to clarify my doubts despite his busy schedules and I consider it as a great opportunity to do my doctoral program under his guidance and to learn from his research expertise.

I am profoundly grateful to Prof. Satoshi Minakata and Prof. Tsuyoshi Inoue for their valuable comments and suggestions on preparation of this thesis.

The members of our laboratory also have been very kind enough to extend their help at various phases of this research, whenever I approached them, and I do hereby acknowledge all of them. I thank assistant Prof. Urara Hasegawa for her valuable suggestions and concise comments on my research. When I meet with difficulties, she always helps me. I also thank assistant Prof. Takashi Tsujimoto for his kind help and support. I am grateful to Dr. Andre Vandervlies, Dr. Didi Derks and Dr. Mahasweta Nandi for their expert advices and valuable help.

I deeply thank for the support from Prof. Nobuhito Imanaka and Associate Prof. Shinji Tamura for the measurement of XRD.

I thank my senior, Dr. Yuanrong Xin. She is also my best friend in Japan. She has accompanied with me for more than 3 years. We did the stimulating discussions, worked together before deadlines, and had all the fun in the last 3 years. And I also give my thanks to Dr. Jingyu Shan for her kind help and suggestions of my research and life.

I thank my fellow labmates in Uyama laboratory: Mr. Takashi Fujimoto, Mr. Keisuke Okada, Ms. Sungbin Park, Mr. Nao Hosoda, Ms. Hyunhee Shim, Ms. Wenjuan Han, Mr. Boxing Zhang, Mr. Tengjiao Wang, Mr. Guowei Wang, Mr. Qinghui Zhang, Mr. Haotian Wang, Ms. Hitomi Fukuda and all the members in Uyama laboratory for their accompany and kind help.

Thanks to Chinese Government Scholarship for founding my academic training studies and my stay in Japan.

Last but not the least, I would like to thank my family. My parents, Chuanming Sun and Luming Zhu, gave birth to me and support me spiritually throughout my life. My husband, Wei Wang, whose love and encouragement allows me to finish this journey.

December 2012

Xiaoxia Sun